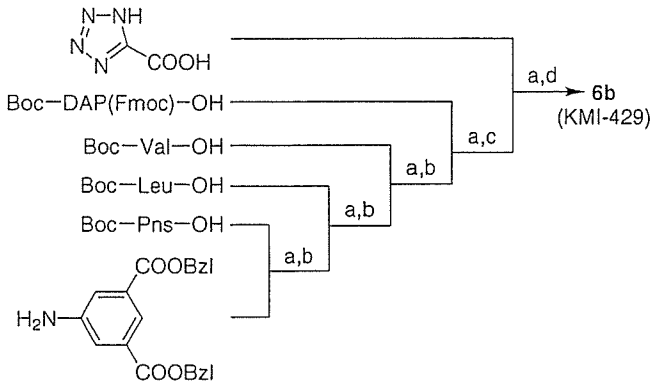

Scheme 2. Reagents and conditions: (a) EDC·HCl, HOBt/DMF; (b) 4M HCl/dioxane; (c) 20% Et_2NH/DMF; (d) TMS-Br, thioanisole, *m*-cresol/TFA.

respectively. The final deprotection of the Boc and benzyl groups using trimethylbromosilane (TMS-Br), thioanisole, and *m*-cresol in TFA and subsequent purification by preparative RP-HPLC gave the desired inhibitor **6b**.

3. Results and discussion

3.1. Stability of KMI-300 (1b) and KMI-358 (2b)

Since the small-sized BACE1 inhibitors, **1b–3b**, showed unstable features, we investigated the mechanism and kinetics for the unstability. It seems that by-products are formed from the isomerization via oxalyl migration. Thus we synthesized the α-oxalyl isomers **1a** and **2a**, corresponding to **1b** and **2b**, respectively, which contained a β-oxalyl DAP group. The HPLC analysis and mass spectra showed that compounds **1a** and **2a** are identical to the by-products of **1b** and **2b**, respectively. Next, we monitored the isomerization of **1b**, **2b**, **1a**, and **2a** in various solvents by HPLC. Compounds **1b**, **2b**, **1a**, and **2a** showed a time-dependent isomerization to an equilibrium mixture (Fig. 4). A slower migration is observed in an aqueous solvent, for example, PBS (phosphate-buffered saline, pH 7.4), than in organic solvents such as MeOH and DMSO. Though the β-isomers (**1b** and **2b**) and α-isomers (**1a** and **2a**), respectively, were isomerized to reach the same equilibrium ratio under the same conditions, the equilibrium ratio and migration rate are dependent on the solvents and the chemical structure of the compounds. Abegaz et al. indicated that the migration rate of oxalyl-DAPs is influenced by the rotamers in the solvents.[19] The difference between α-*N* to β-*N* and β-*N* to α-*N* oxalyl migration rates might determine the equilibrium ratio. Recently, we reported on the water-soluble prodrugs of HIV-1 protease inhibitors based on *O*→*N* intramolecular acyl migration[21–24] and the kinetic study in different solvents.[23,24] These prodrugs could be converted to the parent drugs via a 'five-membered ring intermediate' under physiological conditions. This mechanism via a five-membered ring intermediate, permitted two equilibrium constants, is consistent with the above findings.

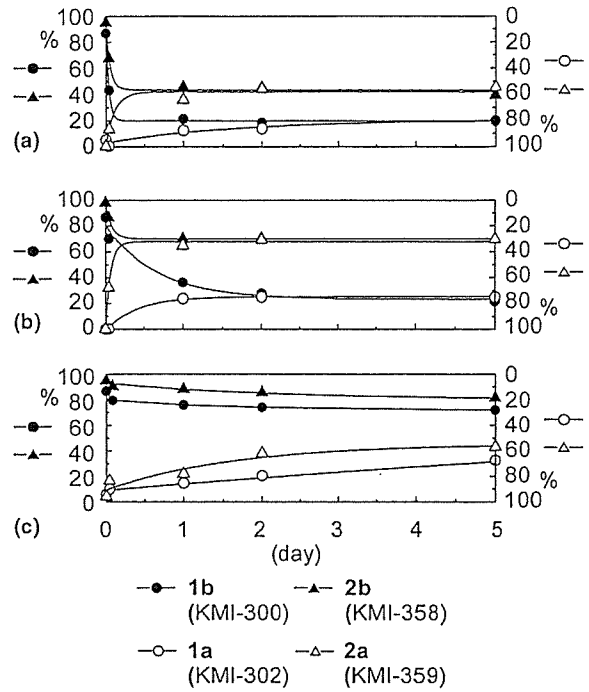

Figure 4. Stability of KMI compounds containing α- or β-oxalyl-DAP residue at the P_4 position in MeOH (a), DMSO (b), or pH 7.4 PBS (c). To unify the β-isomer's ratio to upward direction in the graph, the *y*-axis direction of α-isomers (**1a** and **2a**) was reversed.

3.2. Stability and BACE1 inhibitory activity of KMI-404 (4b), KMI-420 (5b), and KMI-429 (6b)

To improve the stability of BACE1 inhibitors **1b–3b**, we replaced the oxalyl group with the 1*H*-tetrazole-5-carbonyl group. The stability of the tetrazole-type BACE1 inhibitors **4b** (KMI-404), **5b** (KMI-420), and **6b** (KMI-429), which correspond to **1b–3b**, respectively, was verified by HPLC. **4b–6b** showed no isomerization in PBS (pH 7.4), MeOH and DMSO over a period up to 5 days.

As shown in Table 1, the BACE1 inhibitory activities of β-*N*-tetrazole-5-carbonyl-type inhibitors **4b–6b** were enhanced over β-*N*-oxalyl-type inhibitors **1b–3b**, respectively. The α-isomers **1a**, **2a**, **4a**, and **5a** showed weaker BACE1 inhibitory activities than the corresponding

Table 1. BACE1 inhibitory activity

Compd (KMI No.)	BACE1 inhibition (%)		IC_{50} (nM)
	At 2 μM	At 0.2 μM	
1b (KMI-300)	96.7	57.6	84
2b (KMI-358)	98.4	85.5	16
3b (KMI-370)	99.8	96.7	4.7
1a (KMI-302)	75.2	—	—
2a (KMI-359)	87.9	58.6	—
4b (KMI-404)	93.0	73.1	—
5b (KMI-420)	99.0	87.1	8.2
6b (KMI-429)	100	98.1	3.9
4a (KMI-405)	23.2	—	—
5a (KMI-602)	~0	—	—

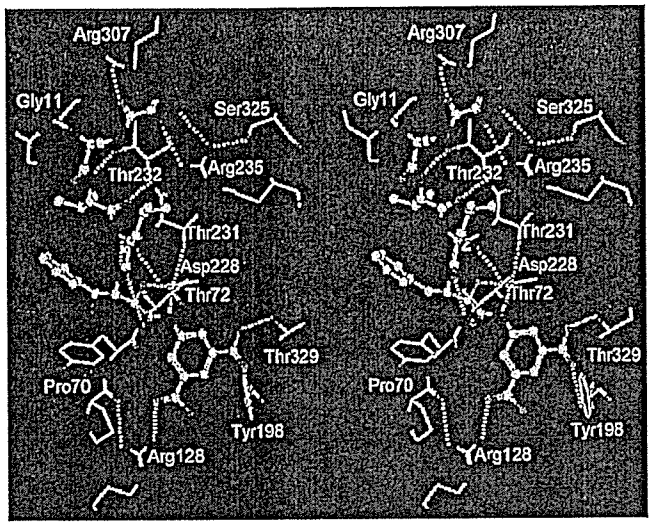

Figure 5. Modeled structure of BACE1 (skeleton model)-**6b** KMI-429 (ball and stick model) complex based on the crystal structure of BACE1 bound to OM99-2.[25] White dashed lines indicate hydrogen bonds to the inhibitor.

β-isomers **1b**, **2b**, **4b**, and **5b**, respectively. As compared with **4a** and **5a** showing no isomerization, relatively high activities of **1a** and **2a** are probably due to the activities of the corresponding β-isomers **1b** and **2b** formed partially by the isomerization of **1a** and **2a** during incubation in this assay. The IC_{50} values of **5b** and **6b** were improved as compared to those of **2b** and **3b**, respectively.

As shown in Figure 5, the tetrazole ring, which is slightly larger than a carboxylic acid, allows the formation of hydrogen bonds to both Arg235 and Arg307 residues of BACE1. Moreover, as previously described,[12] compound **3b**, which contains two carboxylic groups at the P_1' position, exhibited a higher BACE1 inhibitory activity than compound **2b**, which contains a carboxylic group at the P_1' position. Similarly, compound **6b** exhibited higher BACE1 inhibitory activity than compound **5b**. The two carboxylic groups at the P_1' position of compound **6b** allow the formation of rigid hydrogen bonds in BACE1 as shown in Figure 5. As described above, it seems that the acidic functional groups at the P_4 (as an isostere of the carboxylic group) and P_1' sites are important for enhancing BACE1 inhibitory activity.

4. Conclusion

We found that replacing the labile β-*N*-oxalyl-DAP group of **2b** (KMI-358) and **3b** (KMI-370) with a 1*H*-tetrazole-5-carbonyl group resulted in more potent and chemically stable BACE1 inhibitors, **5b** (KMI-420) and **6b** (KMI-429). Replacing carboxylic acid with bioisostere, such as tetrazole ring, is expected to enhance the membrane permeability, which is considered to be a key issue in developing AD's drugs based on the 'amyloid hypothesis'.[26–29]

Acknowledgements

This research was supported in part by the Frontier Research Program and the 21st century COE program of the Ministry of Education, Science and Culture of Japan, and grants from the Ministry of Education, Science and Culture of Japan.

References and notes

1. Selkoe, D. J. *Neuron* **1991**, *6*, 487.
2. Selkoe, D. J. *Nature* **1999**, *399*, A23.
3. Sinha, S.; Lieberburg, I. *Proc. Natl. Acad. Sci. U.S.A.* **1999**, *96*, 11049.
4. Vassar, R.; Bennett, B. D.; Babu-Khan, S.; Kahn, S.; Mendiaz, E. A.; Denis, P.; Teplow, D. B.; Ross, S.; Amarante, P.; Loeloff, R.; Luo, Y.; Fisher, S.; Fuller, J.; Edenson, S.; Lile, J.; Jarosinski, M. A.; Biere, A. L.; Curran, E.; Burgess, T.; Louis, J. C.; Collins, F.; Treanor, J.; Rogers, G.; Citron, M. *Science* **1999**, *286*, 735.
5. Yan, R.; Bienkowski, M. J.; Shuck, M. E.; Miao, H.; Tory, M. C.; Pauley, A. M.; Brashier, J. R.; Stratman, N. C.; Mathews, W. R.; Buhl, A. E.; Carter, D. B.; Tomasselli, A. G.; Parodi, L. A.; Heinrikson, R. L.; Gurney, M. E. *Nature* **1999**, *402*, 533.
6. Sinha, S.; Anderson, J. P.; Barbour, R.; Basi, G. S.; Caccavello, R.; Davis, D.; Doan, M.; Dovey, H. F.; Frigon, N.; Hong, J.; Jacobson-Croak, K.; Jewett, N.; Keim, P.; Knops, J.; Lieberburg, I.; Power, M.; Tan, H.; Tatsuno, G.; Tung, J.; Schenk, D.; Seubert, P.; Suomensaari, S. M.; Wang, S.; Walker, D.; Zhao, J.; McConlogue, L.; John, V. *Nature* **1999**, *402*, 537.
7. Hussain, I.; Powell, D.; Howlett, D. R.; Tew, D. G.; Meek, T. D.; Chapman, C.; Gloger, I. S.; Murphy, K. E.; Southan, C. D.; Ryan, D. M.; Smith, T. S.; Simmons, D. L.; Walsh, F. S.; Dingwall, C.; Christie, G. *Mol. Cell. Neurosci.* **1999**, *14*, 419.
8. (a) Ghosh, A. K.; Shin, D.; Downs, D.; Koelsch, G.; Lin, X.; Ermolieff, J.; Tang, J. *J. Am. Chem. Soc.* **2000**, *122*, 3522; (b) Ghosh, A. K.; Bilcer, G.; Harwood, C.; Kawahara, R.; Shin, D.; Hussain, K. A.; Hong, L.; Loy, J. A.; Nguyen, C.; Koelsch, G.; Ermolieff, J.; Tang, J. *J. Med. Chem.* **2001**, *44*, 2865.
9. Tung, J. S.; Davis, D. L.; Anderson, J. P.; Walker, D. E.; Mamo, S.; Jewett, N.; Hom, R. K.; Sinha, S.; Thorsett, E. D.; John, V. *J. Med. Chem.* **2002**, *45*, 259.
10. Tamamura, H.; Kato, T.; Otaka, A.; Fujii, N. *Org. Biomol. Chem.* **2003**, *1*, 2468.
11. Shuto, D.; Kasai, S.; Kimura, T.; Liu, P.; Hidaka, K.; Hamada, T.; Shibakawa, S.; Hayashi, Y.; Hattori, C.; Szabo, B.; Ishiura, S.; Kiso, Y. *Bioorg. Med. Chem. Lett.* **2003**, *13*, 4273.
12. Kimura, T.; Shuto, D.; Kasai, S.; Liu, P.; Hidaka, K.; Hamada, T.; Hayashi, Y.; Hattori, C.; Asai, M.; Kitazume, S.; Saido, T. C.; Ishiura, S.; Kiso, Y. *Bioorg. Med. Chem. Lett.* **2004**, *14*, 1527.
13. Mimoto, T.; Imai, J.; Tanaka, S.; Hattori, N.; Takahashi, O.; Kisanuki, S.; Nagano, Y.; Shintani, M.; Hayashi, H.; Akaji, K.; Kiso, Y. *Chem. Pharm. Bull.* **1991**, *39*, 2465.
14. Mimoto, T.; Imai, J.; Tanaka, S.; Hattori, N.; Kisanuki, S.; Akaji, K.; Kiso, Y. *Chem. Pharm. Bull.* **1991**, *39*, 3088.
15. Murti, V. V. S.; Seshadri, T. R.; Venkitasubramanian, T. A. *Phytochemistry* **1964**, *3*, 73.
16. Rao, S. L. N.; Adiga, P. R.; Sarma, P. S. *Biochemistry* **1964**, *3*, 432.

17. Spencer, P. S.; Roy, D. N.; Ludolph, A.; Hugon, J.; Dwivedi, M. P.; Schaumburg, H. H. *Lancet* **1986**, *11*, 1066.
18. Bell, E. A.; O'Donovan, J. P. *Phytochemistry* **1966**, *5*, 1211.
19. Abegaz, B. M.; Nunn, P. B.; De Bruyn, A.; Lambein, F. *Phytochemistry* **1993**, *33*, 1121.
20. Kohara, Y.; Kubo, K.; Imamiya, E.; Wada, T.; Inada, Y.; Naka, T. *J. Med. Chem.* **1996**, *39*, 5228.
21. Kiso, Y.; Matsumoto, H.; Yamaguchi, S.; Kimura, T. *Lett. Pept. Sci.* **1999**, *6*, 275.
22. Hamada, Y.; Ohtake, J.; Sohma, Y.; Kimura, T.; Hayashi, Y.; Kiso, Y. *Bioorg. Med. Chem.* **2002**, *10*, 4155.
23. Hamada, Y.; Matsumoto, H.; Kimura, T.; Hayashi, Y.; Kiso, Y. *Bioorg. Med. Chem. Lett.* **2003**, *13*, 2727.
24. Hamada, Y.; Matsumoto, H.; Yamaguchi, S.; Kimura, T.; Hayashi, Y.; Kiso, Y. *Bioorg. Med. Chem.* **2004**, *12*, 159.
25. Hong, L.; Koelsch, G.; Lin, X.; Wu, S.; Terzyan, S.; Ghosh, A. K.; Zhang, X. C.; Tang, J. *Science* **2000**, *290*, 150.
26. Sipe, J. D. *Annu. Rev. Biochem.* **1992**, *61*, 947.
27. Selkoe, D. J. *Ann. N.Y. Acad. Sci.* **2000**, *924*, 17.
28. Steiner, H.; Capell, A.; Leimer, U.; Haass, C. *Eur. Arch. Psychiatric Clin. Neurosci.* **1999**, *249*, 266.
29. Selkoe, D. J. *Ann. Med.* **1989**, *21*, 73.

THE JOURNAL OF BIOLOGICAL CHEMISTRY Vol. 279, No. 13, Issue of March 26, pp. 12355–12362, 2004
Printed in U.S.A.

High Level Expression of Human Immunodeficiency Virus Type-1 Vif Inhibits Viral Infectivity by Modulating Proteolytic Processing of the Gag Precursor at the p2/Nucleocapsid Processing Site*

Received for publication, November 12, 2003, and in revised form, January 6, 2004
Published, JBC Papers in Press, January 13, 2004, DOI 10.1074/jbc.M312426200

Hirofumi Akari‡§, Mikako Fujita¶, Sandra Kao‡, Mohammad A. Khan‡, Miranda Shehu-Xhilaga‡, Akio Adachi¶, and Klaus Strebel‡‖

From the ‡Laboratory of Molecular Microbiology, NIAID, National Institutes of Health, Bethesda, Maryland 20892-0460, §Tsukuba Primate Center for Medical Science, The National Institute of Infectious Diseases, Ibaraki 305-0843, Japan, and the ¶Department of Virology, The University of Tokushima Graduate School of Medicine, Tokushima 770-8503, Japan

The human immunodeficiency virus type-1 Vif protein has a crucial role in regulating viral infectivity. However, we found that newly synthesized Vif is rapidly degraded by cellular proteases. We tested the dose dependence of Vif in non-permissive H9 cells and found that Vif, when expressed at low levels, increased virus infectivity in a dose-dependent manner. Surprisingly, however, the range of Vif required for optimal virus infectivity was narrow, and further increases in Vif severely reduced viral infectivity. Inhibition of viral infectivity at higher levels of Vif was cell type-independent and was associated with an accumulation of Gag-processing intermediates. Vif did not act as a general protease inhibitor but selectively inhibited Gag processing at the capsid and nucleocapsid (NC) boundary. Identification of Vif variants that were efficiently packaged but were unable to modulate Gag processing suggests that Vif packaging was necessary but insufficient for the production of 33- and 34-kDa processing intermediates. Interestingly, these processing intermediates, like Vif, associated with viral nucleoprotein complexes more rigidly than mature capsid and NC. We conclude that virus-associated Vif inhibits processing of a subset of Gag precursor molecules at the p2/NC primary cleavage site. Modulation of processing of a small subset of Gag molecules by physiological levels of Vif may be important for virus maturation. However, the accumulation of such processing intermediates at high levels of Vif is inhibitory. Thus, rapid intracellular degradation of Vif may have evolved as a mechanism to prevent such inhibitory effects of Vif.

The human immunodeficiency virus type-1 (HIV-1)[1] Vif protein is essential for viral replication in non-permissive cells such as primary CD4+ T lymphocytes and macrophages as well as some T cell lines including H9 and CEM cells (for review, see Refs. 1 and 2). Vif-defective viruses produced from non-permissive cells are defective at an early postentry step of infection and are unable to complete reverse transcription and integration (3–9). In fibroblasts and most T cell lines, however, Vif is not required for the production of infectious HIV-1. This cell type-dependent requirement for Vif implied the involvement of host factor(s). Indeed, the recent identification of CEM15 (APOBEC3G) as a cellular inhibitor of HIV replication (10) confirmed earlier speculations on the existence of an inhibitory factor in non-permissive cell types (11, 12). APOBEC3G was subsequently found to induce hypermutation of the HIV genome by deaminating cytidine residues on the viral minus-strand cDNA resulting in the introduction of guanosine to adenosine mutations in the HIV genome (13–16). Subsequent reports suggested a role of Vif in the inhibition of APOBEC3G packaging into virus particles (17–21). The mechanism of APOBEC3G exclusion from virions, however, remains under investigation. Some reports suggest that Vif induces degradation of APOBEC3G (20, 21), whereas others report an effect on APOBEC3G translation (17, 19) or both (18).

While most current models propose an intracellular interaction of Vif with APOBEC3G, Vif is also packaged into virions. Virus particles produced from acutely infected cells incorporate 30–100 copies of Vif (22). In fact, packaging of Vif is specific and requires the interaction of Vif with the viral genomic RNA and the nucleocapsid (NC) domain of the Gag precursor (23). Moreover, virus-associated Vif is partially cleaved by the viral protease (PR) (24). Interestingly, mutations at the processing site that inhibited Vif processing inhibited Vif function, whereas mutations that did not interfere with Vif processing also did not affect Vif function (24). While these findings suggested an important role of virus-associated Vif in virions (24), its specific role remains under investigation.

In the current study we report that newly synthesized Vif is rapidly degraded in transiently transfected HeLa cells with a half-life of less than 30 min. We found that the presence or absence of APOBEC3G had no significant effect on the degradation kinetics of Vif. Based on recent reports demonstrating an interaction of Vif with APOBEC3G (17, 21, 25), we postulated that Vif enhances viral infectivity in a dose-dependent and saturable manner. Accordingly, increasing levels of Vif were expected to result in an increase in viral infectivity reaching a plateau of maximal infectivity once saturating amounts of Vif were reached or exceeded. Furthermore, increasing the amounts of Vif in permissive cell types was not expected to affect viral infectivity, as virus production in such cell types is Vif-independent due to the lack of APOBEC3G in such cells. As expected, physiological expression of Vif increased viral infec-

* This work was supported in part by a grant from the National Institutes of Health Intramural AIDS Targeted Antiviral Program (to K. S.). The costs of publication of this article were defrayed in part by the payment of page charges. This article must therefore be hereby marked "*advertisement*" in accordance with 18 U.S.C. Section 1734 solely to indicate this fact.

‖ To whom correspondence should be addressed: NIAID, National Institutes of Health, 4/312, 4 Center Dr., MSC 0460, Bethesda, MD 20892-0460. Tel.: 301-496-3132; Fax: 301-402-0226; E-mail: kstrebel@nih.gov.

[1] The abbreviations used are: HIV-1, human immunodeficiency virus type-1; NC, nucleocapsid; CA, capsid; VSV-G, vesicular stomatitis virus glycoprotein G; MA, matrix; CHAPS, 3-[(3-cholamidopropyl)dimethylammonio]-1-propanesulfonic acid; PR, protease.

tivity in non-permissive cell types in a dose-dependent manner. Surprisingly, however, the amounts of Vif required for maximal effect exhibited a narrow window, and further increases in Vif levels did not result in a plateau of maximal viral infectivity but instead increasingly suppressed viral infectivity irrespective of the producer cell type. We investigated the mechanistic basis of this phenomenon and found that Vif suppresses processing of the Gag precursor at the p2/NC primary cleavage site. The resulting accumulation of 33- and 34-kDa Gag intermediates composed of CA-p2-NC and CA-p2-NC-p1 was found to inhibit viral infectivity. These results provide evidence that virus-associated Vif has the ability to interact with Gag precursor molecules and to modulate Gag maturation. However, Gag maturation is a highly ordered process, and accumulation of excessive amounts of processing intermediates due to high level expression of Vif is detrimental to virus infectivity.

EXPERIMENTAL PROCEDURES

Plasmids—The full-length HIV-1 molecular clone pNL4-3 was used for the production of wild type infectious virus (26). Construction of its variants pNL43-K1 (Env-defective) or pNL4-3vif(−) (Vif-defective) was described previously (27, 28). An Env- and Vif-defective variant, pNL43-K1.vif(−), was constructed by introducing a frameshift mutation in *env* at a KpnI site in pNL4-3vif(−). Plasmid pHCMV-G contains the vesicular stomatitis virus glycoprotein G (VSV-G) gene expressed from the immediate early gene promoter of human cytomegalovirus (29) and was used for the production of VSV-G pseudotypes. Construction of the APOBEC3G expression vector pHIV-Apo3G is described elsewhere (19). Expression of APOBEC3G from pHIV-Apo3G is under the control of the HIV-1 long terminal repeat and thus requires Tat for expression. For expression of Vif in *trans*, the subgenomic expression vector pNL-A1 (30) was used. A Vif-defective variant of pNL-A1, pNL-A1vif(−), was used as a control. Vif deletion mutants VifΔD (deletion of residues 23–43), VifΔF (deletion of residues 23–74), and VifΔI (deletion of residues 4–45) were created by two-step PCR amplification. PCR products were column-purified; appropriate pairs were mixed at equimolar ratios and used as templates for a second round of amplification using flanking primers. Final PCR products were cloned into pNL-A1 between the BssHII and EcoRI sites.

Cells—H9 and LuSIV cells were cultured in RPMI 1640 medium supplemented with 10% fetal bovine serum, L-glutamine, and antibiotics. HeLa cells were maintained in complete Dulbecco's modified Eagle's medium supplemented with 10% fetal bovine serum, L-glutamine, and antibiotics.

Transfection and Analysis of Viral Proteins—H9 cells (4×10^6) were transfected by electroporation with 10 μg each of pNL43-K1 or pNL43-K1.vif(−) and 10 μg of pNL-A1 or pNL-A1vif(−). The culture supernatants were harvested 24 h after transfection, filtered through 0.45-μm filters, and concentrated by ultracentrifugation through 20% sucrose for 1 h at 25,000 rpm using an SW41 rotor (Beckman Instruments). Alternatively, HeLa cells (5×10^6) were transfected with 2 μg each of variants of pNL4-3 and pNL-A1 using LipofectAMINE PLUS™ (Invitrogen). Culture supernatants and cells were harvested 24 h later. Cell and viral lysates were analyzed by immunoblotting as described previously (23) using an HIV-1-infected patient serum (APS) and antibodies against Vif (28), NC (kindly provided by Robert Gorelick), reverse transcriptase (Intracell), p24 capsid, and matrix (MA) (provided by S. Zolla-Pazner and P. Spearman, respectively, and obtained through the National Institutes of Health AIDS Research and Reference Reagent Program (31, 32)).

Pulse/Chase Analysis of Vif—Transfected cells were metabolically labeled for 10 min with [^{35}S]methionine (2 mCi/ml; ICN Biomedical, Inc., Costa Mesa, CA). After the labeling, cells were washed once with phosphate-buffered saline to remove free isotope and suspended in complete RPMI containing all amino acids and 10% fetal bovine serum. Cells were incubated for various times at 37 °C as indicated in the text. Cells were then pelleted and stored at −80 °C. Cell pellets were subsequently extracted with CHAPS buffer (50 mM Tris-hydrochloride, pH 8.0, 5 mM EDTA, 100 mM NaCl, and 0.5% (v/v) CHAPS (3-[(3-cholamidopropyl)dimethylammonio]-1-propanesulfonic acid)) supplemented with 0.2% deoxycholate, incubated on ice for 5 min, vortexed, and pelleted for 3 min at 15,000 × *g*. Proteins present in the supernatant were used for immunoprecipitation with a Vif-specific polyclonal antibody (Vif93) (28). Immunoprecipitated proteins were solubilized by boiling in sample buffer and separated by SDS-PAGE. Radioactive bands were visualized by fluorography, and quantitation was performed using a Fuji BAS 2000 Bio-Image analyzer.

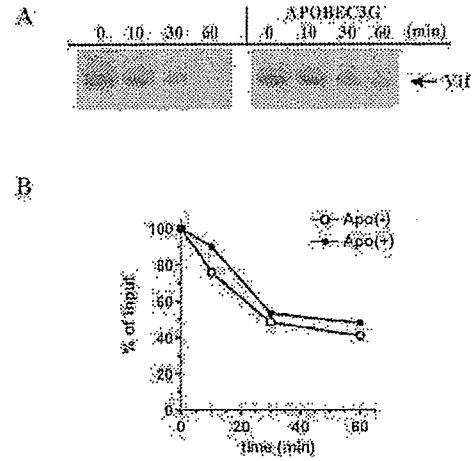

FIG. 1. **Newly synthesized Vif is rapidly degraded.** *A*, HeLa cells were transfected with pNL-A1 (4 μg) and a control vector, pHIV-T4 (1 μg) or pNL-A1 (4 μg) plus pHIV-Apo3G (1 μg). Cells were collected 24 h after transfection, labeled for 10 min with [^{35}S]methionine, and chased for up to 60 min as indicated *above the lanes*. Cell lysates were prepared as described under "Experimental Procedures" and precipitated with a Vif-specific polyclonal antibody. Vif proteins were identified by SDS-PAGE followed by fluorography. *B*, Vif-specific bands shown in *A*, respectively, were quantified using a Fuji BAS 2000 Phospho-Imager. Signals were calculated relative to the input value (time 0 = 100%) and plotted as a function time.

Single-round Viral Infectivity Analysis—Virus stocks derived from transfected H9 or HeLa cells were used for the infection of LuSIV indicator cells (33). To increase the sensitivity of the assay, viruses were pseudotyped with the vesicular stomatitis virus glycoprotein G. Unlike Nef defects, VSV-G pseudotyping does not rescue Vif defects (3, 34). LuSIV cells (5×10^5) were infected in a 24-well plate with 200–400 μl of unconcentrated virus supernatants. Cells were incubated for 24 h at 37 °C. Cells were then harvested and lysed in 150 μl of Promega 1× reporter lysis buffer (Promega Corp., Madison, WI). To determine the luciferase activity in the lysates, 50 μl of each lysate were combined with luciferase substrate (Promega Corp.) by automatic injection, and light emission was measured for 10 s at room temperature in a luminometer (Optocomp II, MGM Instruments, Hamden, CT).

Step Gradient Analysis—Concentrated virus preparations were treated with 0.1% Triton X-100 (final concentration) and subjected to fractionation by centrifugation through a 20%/60% sucrose step gradient as described previously (23). Three equal fractions were collected as depicted in Fig. 5; the top fraction (fraction 1) contains detergent-soluble viral proteins, fraction 2 is a buffer fraction and should not contain significant amounts of any viral proteins, and fraction 3 contains viral core components that are resistant to extraction with Triton X-100. Aliquots of each fraction were analyzed for viral proteins by immunoblotting.

RESULTS

Newly Synthesized Vif Is Rapidly Degraded—Recent work proposed that Vif induces proteasome-dependent degradation of APOBEC3G (20, 21, 25). Although we and others were unable to verify such Vif-dependent degradation of APOBEC3G (17, 19), we nevertheless wanted to assess the possible impact of APOBEC3G on Vif stability. To address this question, we performed pulse/chase analyses in transiently transfected HeLa cells (Fig. 1). To ascertain coexpression of Vif and APOBEC3G in the same cells, Vif was expressed from the subgenomic expression vector pNL-A1 (30), and APOBEC3G was expressed from the Tat-dependent vector pHIV-Apo3G (19). Transfected HeLa cells were labeled for 10 min with [^{35}S]methionine and chased for up to 60 min as described under "Experimental Procedures." As can be seen in Fig. 1*A*, Vif was rapidly degraded both in the absence and presence of

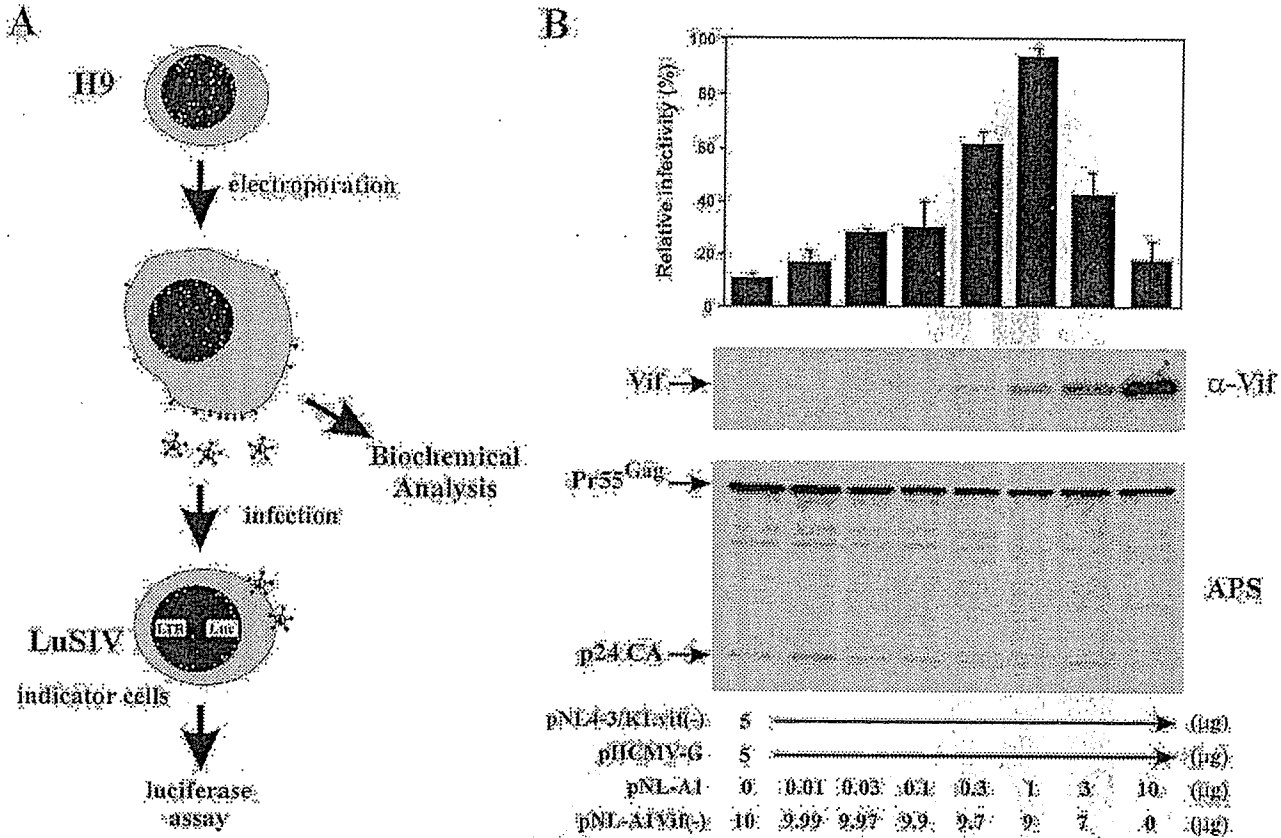

FIG. 2. **Vif is a positive and negative regulator of viral infectivity.** *A*, schematic representation of the experimental procedure. H9 cells are non-permissive and do not support replication of Vif-defective viruses. LuSIV cells are CD4+ indicator cells carrying a luciferase gene under the control of the SIV_{mac239} long terminal repeat (33). *B*, H9 cells were electroporated with constant amounts (5 μg) each of the Vif- and Env-defective pNL43-K1.vif(−) proviral construct and the VSV-G expression vector, pHCMV-G. In addition, increasing amounts of the Vif expression vector pNL-A1 (0–10 μg) were included as indicated at the *bottom*. All samples were adjusted to a total of 20 μg of plasmid DNA using the Vif-defective variant pNL-A1vif( ). Transfected cells and virus-containing supernatants were harvested 24 h after electroporation, and cell lysates were subjected to immunoblot analysis using a Vif-specific antiserum (*α-Vif*) or an HIV-positive patient serum (*APS*). Proteins are identified on the *left*. Virus-containing supernatants were adjusted for equal reverse transcriptase activity (46) and used for the infection of LuSIV indicator cells. Luciferase activity was determined 24 h after infection and used to calculate the relative infectivity of the individual virus stocks (*top*). Maximal infectivity was defined as 100%.

APOBEC3G. Quantitation of the Vif-specific bands (Fig. 1*B*) revealed no difference in the relative decay rates of Vif. Thus, expression of APOBEC3G had no impact on the intracellular stability of Vif. The intracellular site of Vif degradation is under investigation; however, preliminary data suggest the involvement of the cellular proteasome machinery (35).[2]

High Level Expression of Vif in Virus-producing Cells Is Detrimental to HIV-1 Infectivity—The rapid intracellular turnover presumably contributes to the low abundance of Vif in virus-infected cells and limits its packaging into virions. This suggests that Vif may function at very low levels. To determine how much Vif is required for maximal viral infectivity, we examined the dose-dependent effect of Vif on viral infectivity in non-permissive H9 cells. Virus stocks were produced in the presence of increasing amounts of Vif and tested for infectivity in a single-round infection assay. To avoid subsequent rounds of infection, an *env*-defective proviral construct, pNL43-K1.vif(−), was used and pseudotyped with VSV-G. As pNL43-K1.vif(−) is also defective in its *vif* gene, Vif was expressed in *trans* from pNL-A1 (30). This allowed for the controlled expression of increasing amounts of Vif depending on the amounts of pNL-A1 vector transfected. To avoid fluctuations in transfection efficiencies all DNA amounts were equalized by addition of appropriate amounts of a Vif-defective variant of pNL-A1, pNL-A1.vif(−). Cells transfected with constant amounts (5 μg) of pNL43-K1.vif(−) as well as pHCMV-G (5 μg) and increasing amounts of pNL-A1 (0.01–10 μg) were harvested 24 h after electroporation. Cell lysates and virus-containing supernatants were used for biochemical characterization as well as for the infection of LuSIV indicator cells as illustrated in Fig. 2*A*. LuSIV cells were collected 24 h after infection, and luciferase activity in the cell lysates was measured as described under "Experimental Procedures." Luciferase activity was normalized for input virus and expressed as percentage of the activity observed for a Vif-expressing control virus, which was defined as 100% (Fig. 2*B*). At low expression levels, Vif enhanced virus infectivity in a dose-dependent manner reaching a peak of infectivity at 1 μg of cotransfected pNL-A1 plasmid DNA. Surprisingly, however, viral infectivity did not plateau with further increases in Vif, but instead higher levels of Vif resulted in a rapid drop in virus infectivity. In fact, at the highest concentration tested (10 μg of pNL-A1 plasmid), the infectivity of the resulting virus was comparable with that of Vif-defective virus. Western blot analysis confirmed that the levels of Vif expression were directly correlated with the amounts of pNL-A1 plasmid transfected (Fig. 2*B*, *α-Vif*) and that increasing Vif expression did not significantly affect Gag expression (Fig. 2*B*, *APS*). These results demonstrate that the level of Vif required for maximal infectivity has a very narrow optimum and that both

[2] M. Fujita, manuscript in preparation.

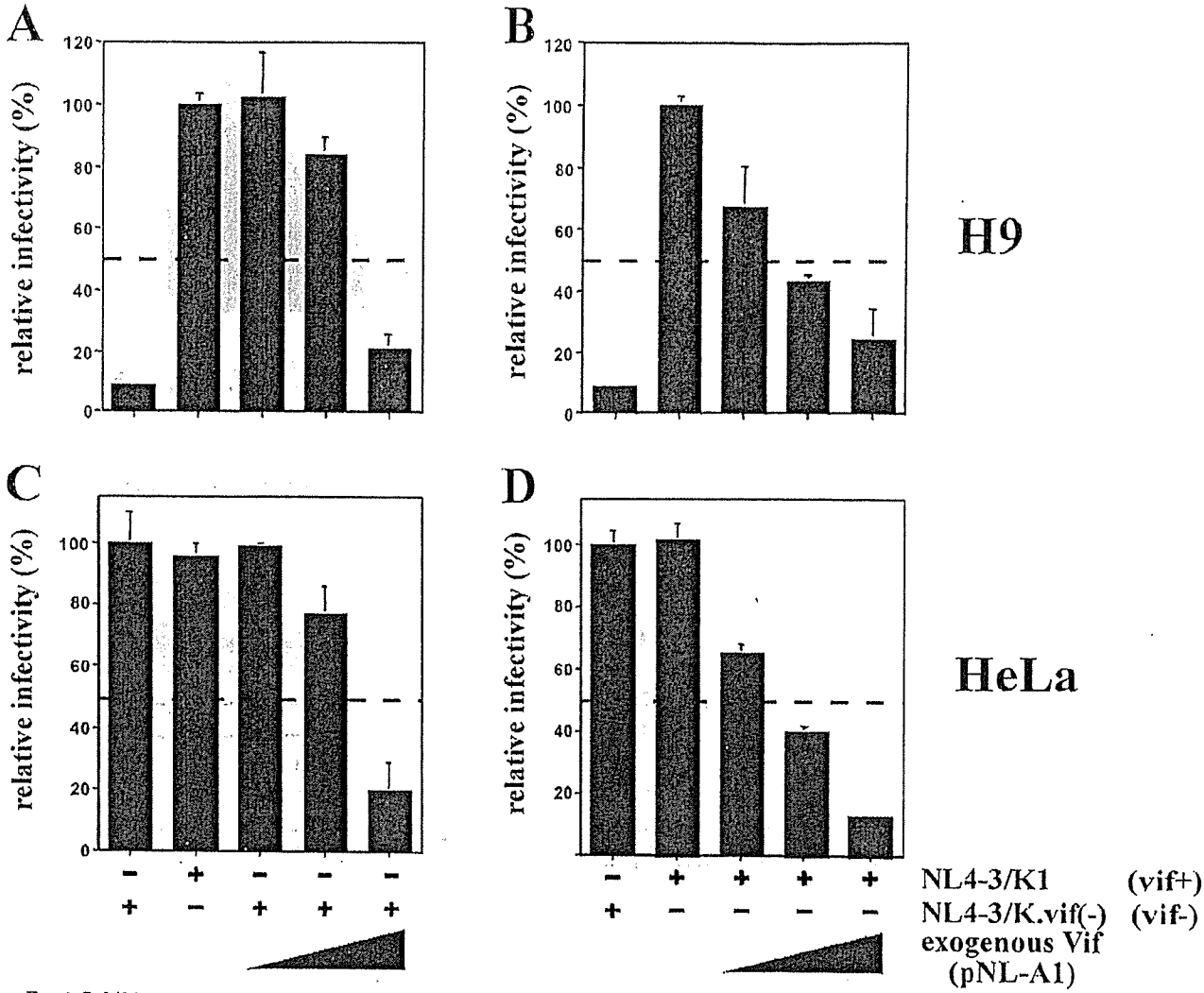

FIG. 3. **Inhibition of virus infectivity at high levels of Vif is cell type-independent.** *A* and *B*, H9 cells were electroporated with increasing amounts (1, 3, or 10 μg) of the Vif-expressing pNL-A1 plasmid DNA, together with a proviral construct and pHCMV-G, essentially as described for Fig. 1. In *A* the Vif- and Env-defective proviral vector pNL43-K1.vif(−) was employed, whereas in *B* a Vif-expressing variant, pNL43-K1, was used. *C* and *D*, HeLa cells were transfected following the same schedule as described for *A* and *B* except that the total amount of DNA was adjusted to 5 μg. The relative ratio of individual plasmids was not changed. Virus-containing supernatants were harvested for all samples 24 h after transfection, normalized for equal reverse transcriptase activity, and used for the infection of LuSIV cells. Viral infectivity was calculated as described for Fig. 1. In all four sets, a Vif-deficient control (*first bar* in each *panel*) and a positive control expressing physiological amounts of Vif (*second bar*) were included. The *dotted line* indicates 50% infectivity.

lower and higher levels of Vif are detrimental to virus infectivity.

Inhibition of Virus Infectivity at High Levels of Vif Is Cell Type-independent—The results from Fig. 2 are unexpected inasmuch as they are inconsistent with a model that simply envisions a role of Vif in the inactivation of cellular inhibitor(s) such as APOBEC3G. To directly examine the requirement of cellular inhibitory factors for the dose-dependent effect of Vif on viral infectivity, we compared the infectivity of virus stocks produced from non-permissive H9 cells and permissive HeLa cells in the presence of increasing amounts of Vif. In addition, to rule out the possibility that the inhibitory effect of Vif seen following overexpression in *trans* is due to the fact that the proviral vector employed in this study carried a defective *vif* gene, we analyzed a Vif-expressing variant (pNL43-K1) in direct comparison to the Vif-defective pNL43-K1.vif(−). H9 cells (Fig. 3, *A* and *B*) and HeLa cells (*C* and *D*) were transfected with increasing amounts (1–10 μg) of pNL-A1 together with fixed amounts (5 μg) of pNL43-K1 or pNL43-K1.vif(−) as indicated in Fig. 3. In addition, a fixed amount (5 μg) of pHCMV-G was included to produce VSV-G-pseudotyped virus stocks. As before, DNA quantities were adjusted to 20 μg in all samples using appropriate amounts of pNL-A1.vif(−) plasmid DNA. Consistent with the results from Fig. 2, physiological levels of Vif supplied in *trans* or in *cis* produced fully infectious virus from both H9 and HeLa cells, and further increase in the amounts of Vif progressively reduced viral infectivity in H9-derived virus (Fig. 3, *A* and *B*). Interestingly, the inhibitory effect of Vif expressed in *cis* and in *trans* appeared to be additive because in the presence of endogenous Vif, smaller amounts of exogenous Vif were necessary for a comparable degree of inhibition (compare *A* and *B* of Fig. 3). These results indicate that the inhibitory effect of high levels of Vif on virus infectivity in Fig. 2 was not due to the lack of a functional *vif* gene.

Surprisingly, very similar results were observed when virus was produced from permissive HeLa cells (Fig. 3, *C* and *D*);

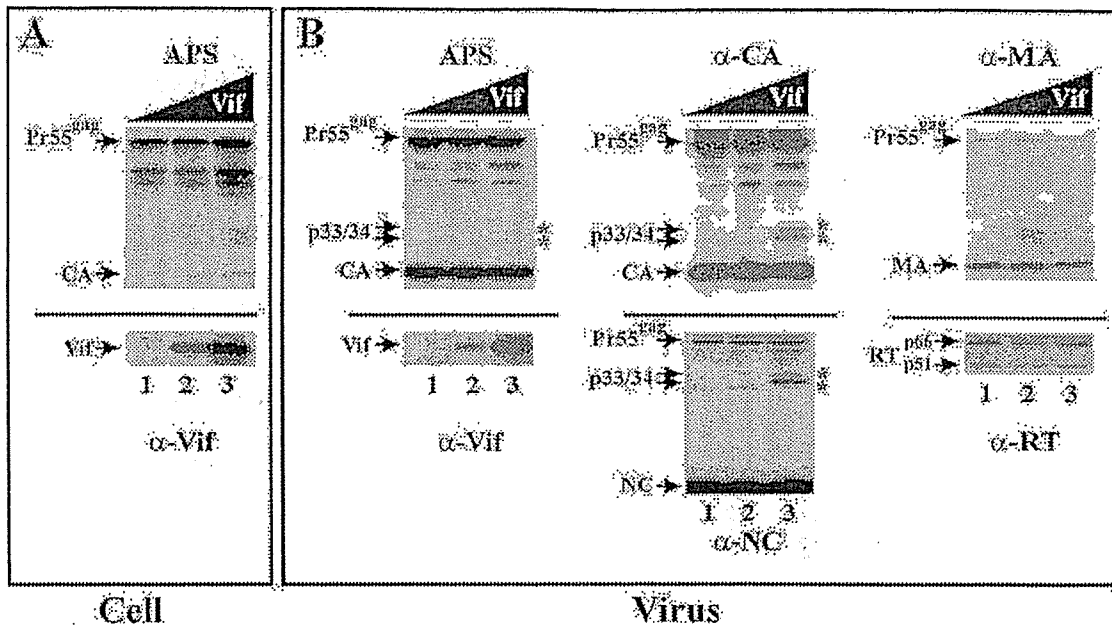

FIG. 4. **High level expression of Vif in H9-derived virus preparations reveals an effect of Vif on Gag maturation that is evident by the appearance of 33- and 34-kDa Gag intermediates.** H9 cells were cotransfected by electroporation with equal amounts of pNL43-K1.vif(−) and pNL-A1vif(−) (*lanes 1*), pNL43-K1 and pNL-A1vif(−) (*lanes 2*), or pNL43-K1 and pNL-A1 (*lanes 3*). Cell lysates (*A*) and viral pellets (*B*) obtained 24 h after transfection were analyzed for viral proteins by immunoblotting using an HIV-positive patient serum (*APS*) or antibodies against Vif (*α-Vif*), capsid (*α-CA*), nucleocapsid (*α-NC*), matrix (*α-MA*), and reverse transcriptase (*α-RT*) as indicated. Relative Vif expression levels are marked at the *top* of each *panel*. *Asterisks* mark the positions of the p33/34 Gag intermediates.

overexpression of Vif in *trans* reduced viral infectivity irrespective of the presence or absence of endogenous Vif. Again, endogenous Vif appeared to have an additive effect suggesting a similar molecular mechanism in both cell types. The fact that high level expression of Vif affected viral infectivity in the absence of cellular inhibitory factors suggests that this effect of Vif is unrelated to the noted inhibition of APOBEC3G and thus reflects a separate activity of Vif.

Vif Modulates Gag Processing during Virus Maturation—To investigate the molecular basis of the Vif-induced inhibition of viral infectivity, we performed a biochemical characterization of virions produced in the presence of varying amounts of Vif. The goal was to identify possible effects of Vif on Gag precursor processing or other effects on the viral protein composition that might explain the altered infectivity. In H9 cells, comparable expression and processing of viral proteins including $Pr55^{gag}$ and CA were detected intracellularly using an HIV-positive patient serum (Fig. 4*A*, *APS*) irrespective of the level of Vif expression (Fig. 4*A*, *α-Vif*). Interestingly, analysis of virus-associated proteins revealed two protein bands of ~33 and 34 kDa, respectively, that were apparent only in viruses produced in the presence of high levels of Vif (Fig. 4*B*, *APS*). Both proteins were also recognized by capsid- (Fig. 4*B*, *α-CA*) and nucleocapsid-specific (Fig. 4*B*, *α-NC*) antisera but not by a matrix-specific antibody (Fig. 4*B*, *α-MA*). The reactivity of p33/34 with CA- and NC-specific antibodies identified these proteins as Gag-processing intermediates composed of CA-p2-NC (p33) or CA-p2-NC-p1 (p34). The p33/34 intermediates were significantly less abundant than mature CA or NC suggesting that they represent a minor component of the virions. Importantly, processing of neither p66/p51 reverse transcriptase nor p17 MA was affected by the high levels of Vif (Fig. 4*B*), indicating that Vif does not act as a general PR inhibitor. In addition, similar Gag-processing intermediates were observed in virus derived from permissive HeLa cells in the presence of high levels of Vif (see Fig. 5). Together, the results

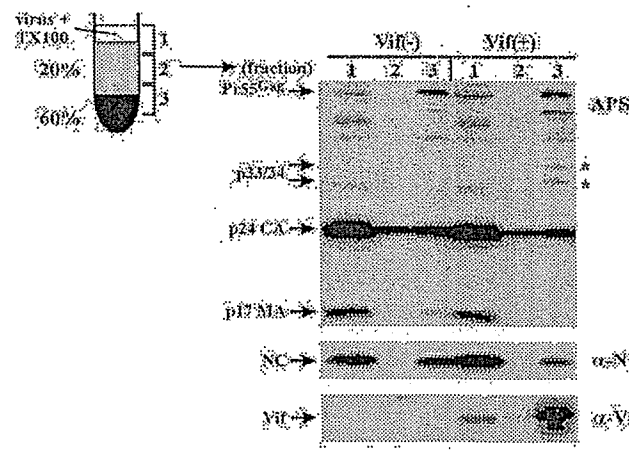

FIG. 5. **Vif and 33- and 34-kDa Gag intermediates copurify with the viral nucleoprotein complex.** HeLa cells were cotransfected with pNL4-3vif(−) and pNL-A1vif(−) (*Vif(−)*) or pNL4-3vif(−) and pNL-A1 (*Vif(+)*). Virus-containing supernatants were concentrated, adjusted to a final concentration of 0.1% Triton X-100, and subjected to sucrose step gradient centrifugation. Three equal fractions were collected as indicated in the diagram. Each fraction was analyzed for viral proteins by immunoblotting using an HIV-positive patient serum (*APS*) or antibodies to NC (*α-NC*) and Vif (*α-Vif*). *Asterisks* indicate the positions of p33/34.

from this experiment demonstrate that Vif modulates Gag processing to produce CA-p2-NC intermediates.

Vif and Gag Intermediates Associate with the Nucleoprotein Complex—Our observation that Vif modulates the maturation of Gag precursor molecules without acting as a general PR inhibitor suggests that Vif might inhibit Gag processing through steric interference. It is likely that such interference is caused by a direct interaction of Vif with the Gag precursor at or near the p2/NC cleavage site. In fact, several previous stud-

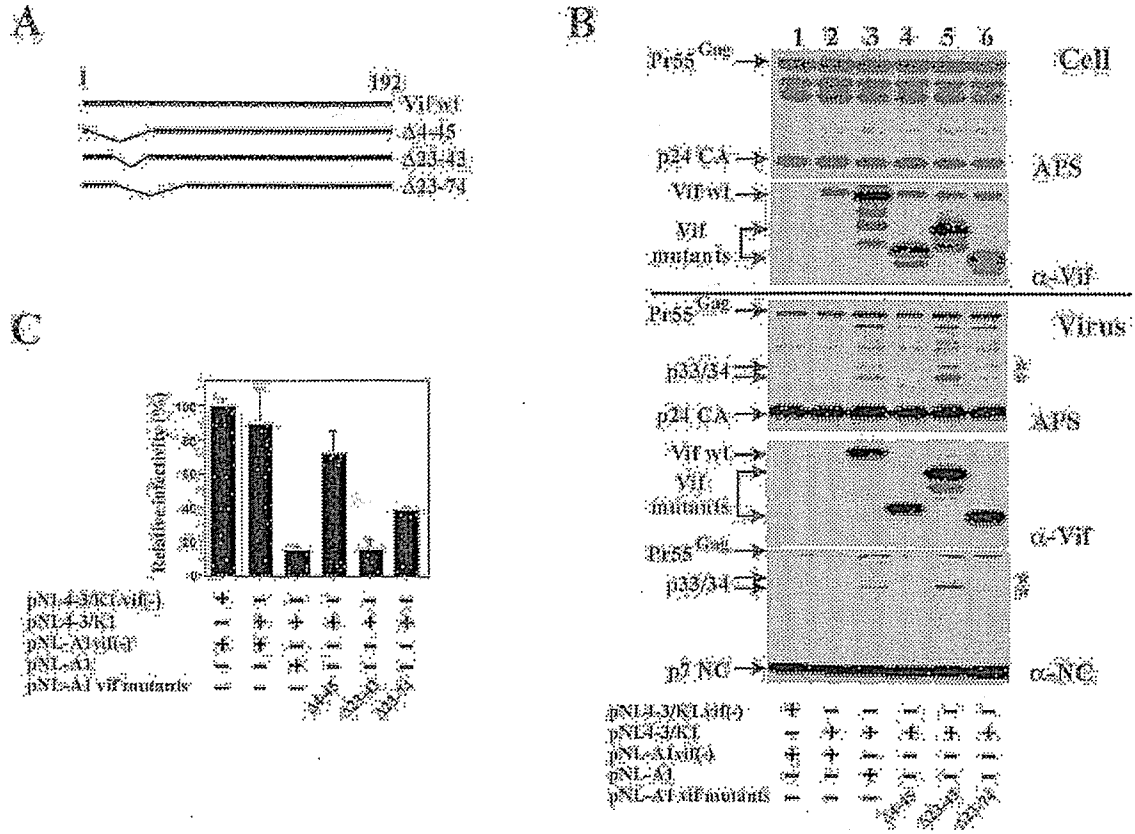

FIG. 6. **Effect of in-frame deletions on the ability of Vif to modulate maturation of Gag precursor molecules.** *A*, schematic diagram of Vif deletion mutants employed in this experiment. The amino acid regions deleted are shown on the *right*. *wt*, wild type. *B*, HeLa cells were cotransfected with equal amounts of pNL43-K1.vif(−) and pNL-A1vif(−) (*lane 1*), pNL43-K1 and pNL-A1vif(−) (*lane 2*), pNL43-K1 and pNL-A1 (*lane 3*), or pNL43-K1 and various pNL-A1-based Vif deletion mutants as indicated (*lanes 4–6*). Cell lysates (*Cell*) and concentrated virus preparations (*Virus*) were harvested 24 h after transfection and analyzed for viral proteins by immunoblotting using APS, anti-Vif, or anti-NC antibodies as indicated on the *right*. Viral proteins are identified on the *left*. *Asterisks* indicate the positions of p33/34. *C*, virus-containing supernatants from *B* were adjusted for equal reverse transcriptase activities and used for the infection of LuSIV indicator cells. Luciferase activity was determined as described under "Experimental Procedures," and the relative infectivity of the virus stocks was calculated.

ies have demonstrated direct interaction of Vif with the viral Gag precursor molecules *in vitro* (36–38). In addition, our recent observation that mutations in the NC zinc finger domains abolish Vif packaging further points to an interaction of Vif and NC (23). Also, virus-associated Vif is stably associated with the viral core, whereas major portions of the mature CA and NC are sensitive to detergent extraction and thus are either not or only loosely associated with the core (23). If maturation of Gag is blocked through steric interference by Vif, we would assume that the resulting intermediates colocalize with Vif in the viral core. To address this issue, viruses obtained from HeLa cells expressing high levels of Vif (Fig. 5, *Vif(+)*) or lacking Vif expression (Fig. 5, *Vif(−)*) were subjected to step gradient centrifugation in the presence of Triton X-100 as reported previously (23). Western blot analysis of individual fractions of the step gradient confirmed the stable association of Vif with the viral core in the insoluble fraction (Fig. 5, *lane 3*, *α-Vif*) as well as the presence of MA and major portions of CA and NC in the soluble fraction (Fig. 5, *lanes 1*). Interestingly, the p33/34 Gag intermediates were resistant to detergent extraction and colocalized with Vif in the viral core fraction (Fig. 5, *lane 3*, *asterisks*) in the presence of Vif. These findings indicate that unlike mature CA and NC products, the Gag p33/34 intermediates are tightly associated with the viral nucleoprotein complex, which also contains the viral genomic RNA, reverse transcriptase, integrase, residual $Pr55^{gag}$, and Vif (23).

Modulation of Gag Processing Requires Packaging of Vif and Involves N-terminal Regions in Vif—In an attempt to determine the domain(s) in Vif contributing to the modulation of proteolytic processing of the Gag precursor molecules, a series of Vif deletion mutants (schematically diagrammed in Fig. 6*A*) was evaluated. As can be seen in Fig. 6*B*, comparable amounts of the wild type and mutant Vif proteins were expressed intracellularly (Fig. 6*B*, *Cell*), indicating that the mutations did not affect steady-state levels of the resulting proteins. All Vif variants were packaged into virions at levels comparable with those of wild type virus (Fig. 6*B*, *Virus*, *α-Vif*). No aberrant Gag intermediates were apparent in the absence of Vif (Fig. 6*B*, *lane 1*, *APS*) or in the presence of physiological levels of Vif (*lane 2*, *APS* and *α-NC*). In contrast, high level expression of wild type Vif resulted in the appearance of the p33/34 intermediates (Fig. 6*B*, *lane 3*, *APS* and *α-NC*; marked by *asterisks*). Deletion of residues 23–43 in Vif did not impair the ability of Vif to modulate Gag processing as shown by the presence of p33/34 at levels comparable with those observed in the presence of wild type Vif (Fig. 6*B*, compare *lanes 3* and *5*, *Virus*, *APS* and *α-NC*). However, deletion of residues 4–45 (Fig. 6*B*, *lane 4*) completely abolished the ability of Vif to modulate Gag processing despite the presence of high levels of this Vif variant in the virus preparation. Finally, deletion of residues 23–74 (Fig. 6*B*, *lane 6*) partially inhibited the ability to modulate Gag maturation. We confirmed that none of these deletions affected the ability of Vif to associate with the nucleoprotein complex

(data not shown). Analysis of viral infectivity revealed an inverse correlation with the amounts of p33/34 detectable in the virus preparations (Fig. 6C). In contrast, there was no correlation between inhibition of viral infectivity and packaging of Vif. All Vif variants were expressed at similar levels and were packaged and associated with the viral nucleoprotein complex with similar efficiency. Taken together, these results support the notion that inhibition of virus infectivity is correlated with the presence of p33/34 Gag intermediates rather than with the amounts of Vif packaged. Our data further demonstrate that sequences in the N-terminal domain of Vif, in particular residues 4–22, are critical for the ability of Vif to inhibit Gag processing at the p2/NC site.

DISCUSSION

Despite the recent identification of a cellular factor whose inhibitory activity must be overcome by Vif to allow for the production of infectious viruses from non-permissive cell types (10), the molecular mechanism of Vif function and its site(s) of action have remained unclear. We now report for the first time on an activity of Vif that requires its presence in virus particles. Our data suggest that Vif modulates the maturation of a small number of Gag and/or Gag-Pol precursor molecules by physically interacting with the Gag or Gag-Pol precursor at or near the primary cleavage site. Such interaction causes the inhibition of or the delay in processing of Gag at the p2/NC cleavage site resulting in the accumulation of small amounts of p33/34 Gag-processing intermediates. Based on their reactivity with both CA- and NC-specific antibodies the p33/34 intermediates were identified as proteins consisting of CA, NC, and one or both of the spacer peptides p1 and p2. Vif did not affect processing at other proteolytic cleavage sites, suggesting that it selectively blocks processing at the CA-NC boundary through steric interference. It is interesting to note that Vif itself is a substrate for proteolytic processing (24), and it is possible that Vif blocks processing of Gag by acting as a decoy for the viral protease.

Processing of the Gag precursor occurs at five different sites to produce at least six mature processing products (39). This process is highly ordered and starts with an initial cleavage at the p2/NC boundary (40). The resulting processing intermediates are then further processed but at a much reduced rate (41). Inhibition of processing at any of the cleavage sites results in the production of non-infectious virions (41, 42). On the other hand, immunoblot analyses of normal infectious HIV-1 virions invariably identify a series of processing intermediates (see Figs. 2 and 6, *Virus, APS*; and 4, *α-CA*) that suggest that Gag processing is incomplete. Notably, most virus preparations contain residual uncleaved $Pr55^{gag}$ precursor. In fact, we noted previously that unlike most mature Gag products, $Pr55^{gag}$ is stably associated with the viral nucleoprotein complex (23). Thus, it is apparent that mature viral particles are composed not only of fully processed Gag and Gag-Pol products but contain residual amounts of Gag precursors and processing intermediates. Whether these processing intermediates have functional significance or are merely signs of an inefficient maturation process remains to be established. However, the noted affinity of $Pr55^{gag}$ as well as the p33/34 intermediates with the viral nucleoprotein complex could imply a role in its formation and/or stabilization.

Vif is known to enhance viral infectivity in a cell type-dependent manner. This phenomenon was recently attributed to the activity of the cellular cytidine deaminase APOBEC3G (13–17). APOBEC3G is packaged into HIV particles where it induces hypermutation of the minus-strand cDNA (10, 14–17). This inhibitory effect of APOBEC3G is counteracted by Vif, which interferes with the packaging of APOBEC3G. How Vif inhibits packaging of APOBEC3G is still under investigation; however, it appears to involve in part a reduction of the intracellular protein levels through proteasome-dependent degradation (18, 20, 21, 25, 35, 43) and requires a physical interaction between the two proteins (17, 18, 21, 35). Thus, like all other viral accessory proteins, Vif appears to be a multifunctional adapter molecule with seemingly opposing effects; binding of Vif to APOBEC3G appears to accelerate its intracellular turnover, whereas the interaction of Vif with the Gag precursor in virions inhibits its proteolytic processing. It is currently unclear whether the domains in Vif required for interaction with APOBEC3G and Gag are the same or map to different regions in the protein. The results from our current study (Fig. 6) suggest that inhibition of Gag processing involves an N-terminal domain in Vif. Although these same mutants were found to also be inactive with respect to APOBEC3G (19), other Vif mutants such as VifΔ23–43 were inactive against APOBEC3G (19) but still inhibited Gag maturation. These results combined with the fact that the effect of Vif on the proteolytic processing of Gag precursors is cell type-independent suggest that the effect of Vif on Gag maturation is mechanistically independent of its neutralization of APOBEC3G. It remains to be investigated whether the interaction of Vif with Gag precursor molecules during or following virus assembly relates to its ability to inhibit packaging of APOBEC3G. This seems possible as the reported reduction of intracellular expression levels of APOBEC3G by Vif does not fully account for the noted exclusion of APOBEC3G from virus particles (17, 19).

The fact that high level expression of Vif is detrimental to viral infectivity confirms that Gag maturation is a carefully balanced process. Thus, rapid degradation of Vif in virus-producing cells may have evolved as a mechanism to preclude the detrimental effects on Gag maturation. Our observation that the accumulation of the CA-p2-NC intermediates is directly correlated with the levels of Vif expression (data not shown) leads us to conclude that similar processing intermediates are produced under physiological conditions but are below the limit of detection in our assay system. The fact that packaging of large quantities of Vif N-terminal deletion mutants did not affect Gag maturation (Fig. 6) suggests that the effect of Vif is specific albeit only detectable by currently available immunoblotting techniques at high levels of Vif. Thus, it is possible that minute quantities of CA-p2-NC- and CA-p2-NC-p1-processing intermediates play an important role in viral infectivity. The fact that such intermediates, unlike their mature products, are stably associated with the nucleoprotein complex raises the possibility that the association of these intermediates with Vif and viral genomic RNA promotes the stability or proper conformation of the viral nucleoprotein complex. Such a function would be consistent with previous reports correlating the lack of Vif with a reduced stability of nucleoprotein complexes (8, 44, 45).

Acknowledgments—We thank Stephan Bour and Eri Miyagi for helpful discussions and Eric Freed for critical comments on the manuscript. We thank Alicia Buckler-White and Ron Plishka for oligonucleotide synthesis and sequence analysis. We acknowledge Mary Karczewski and Claudia Aberham for construction of the Vif mutants and Robert Gorelick, Susan Zolla-Pazner, and Paul Spearman for antibodies. Antibodies to CA and MA were obtained through the National Institutes of Health AIDS Research and Reference Reagent Program.

REFERENCES

1. Bour, S., and Strebel, K. (2000) *Adv. Pharmacol.* 48, 75–120
2. Cullen, B. R. (1998) *Cell* 93, 685–692
3. Akari, H., Uchiyama, T., Fukumori, T., Iida, S., Koyama, A. H., and Adachi, A. (1999) *J. Gen. Virol.* 80, 2945–2949
4. Chowdhury, I. H., Chao, W., Potash, M. J., Sova, P., Gendelman, H. E., and Volsky, D. J. (1996) *J. Virol.* 70, 5336–5345
5. Courcoul, M., Patience, C., Rey, F., Blanc, D., Harmache, A., Sire, J., Vigne, R., and Spire, B. (1995) *J. Virol.* 69, 2068–2074
6. Goncalves, J., Korin, Y., Zack, J., and Gabuzda, D. (1996) *J. Virol.* 70,

8701–8709
7. Reddy, T. R., Kraus, G., Yamada, O., Looney, D. J., Suhasini, M., and Wong-Staal, F. (1995) *J. Virol.* **69**, 3549–3553
8. Simon, J. H., and Malim, M. H. (1996) *J. Virol.* **70**, 5297–5305
9. von Schwedler, U., Song, J., Aiken, C., and Trono, D. (1993) *J. Virol.* **67**, 4945–4955
10. Sheehy, A. M., Gaddis, N. C., Choi, J. D., and Malim, M. H. (2002) *Nature* **418**, 646–650
11. Madani, N., and Kabat, D. (1998) *J. Virol.* **72**, 10251–10255
12. Simon, J. H., Gaddis, N. C., Fouchier, R. A., and Malim, M. H. (1998) *Nat. Med.* **4**, 1397–1400
13. Harris, R. S., Bishop, K. N., Sheehy, A. M., Craig, H. M., Petersen-Mahrt, S. K., Watt, I. N., Neuberger, M. S., and Malim, M. H. (2003) *Cell* **113**, 803–809
14. Zhang, H., Yang, B., Pomerantz, R. J., Zhang, C., Arunachalam, S. C., and Gao, L. (2003) *Nature* **424**, 94–98
15. Mangeat, B., Turelli, P., Caron, G., Friedli, M., Perrin, L., and Trono, D. (2003) *Nature* **424**, 99–103
16. Lecossier, D., Bouchonnet, F., Clavel, F., and Hance, A. J. (2003) *Science* **300**, 1112
17. Mariani, R., Chen, D., Schrofelbauer, B., Navarro, F., Konig, R., Bollman, B., Munk, C., Nymark-McMahon, H., and Landau, N. R. (2003) *Cell* **114**, 21–31
18. Stopak, K., de Noronha, C., Yonemoto, W., and Greene, W. C. (2003) *Mol. Cell* **12**, 591–601
19. Kao, S., Khan, M. A., Miyagi, E., Plishka, R., Buckler-White, A., and Strebel, K. (2003) *J. Virol.* **77**, 11398–11407
20. Sheehy, A. M., Gaddis, N. C., and Malim, M. H. (2003) *Nat. Med.* **9**, 1404–1407
21. Marin, M., Rose, K. M., Kozak, S. L., and Kabat, D. (2003) *Nat. Med.* **9**, 1398–1403
22. Kao, S., Akari, H., Khan, M. A., Dettenhofer, M., Yu, X. F., and Strebel, K. (2003) *J. Virol.* **77**, 1131–1140
23. Khan, M. A., Aberham, C., Kao, S., Akari, H., Gorelick, R., Bour, S., and Strebel, K. (2001) *J. Virol.* **75**, 7252–7265
24. Khan, M. A., Akari, H., Kao, S., Aberham, C., Davis, D., Buckler-White, A., and Strebel, K. (2002) *J. Virol.* **76**, 9112–9123
25. Yu, X., Yu, Y., Liu, B., Luo, K., Kong, W., Mao, P., and Yu, X. F. (2003) *Science* **302**, 1056–1060
26. Adachi, A., Gendelman, H. E., Koenig, S., Folks, T., Willey, R., Rabson, A., and Martin, M. A. (1986) *J. Virol.* **59**, 284–291
27. Bour, S., and Strebel, K. (1996) *J. Virol.* **70**, 8285–8300
28. Karczewski, M. K., and Strebel, K. (1996) *J. Virol.* **70**, 494–507
29. Yee, J. K., Miyanohara, A., LaPorte, P., Bouic, K., Burns, J. C., and Friedmann, T. (1994) *Proc. Natl. Acad. Sci. U. S. A.* **91**, 9564–9568
30. Strebel, K., Daugherty, D., Clouse, K., Cohen, D., Folks, T., and Martin, M. A. (1987) *Nature* **328**, 728–730
31. Gorny, M. K., Gianakakos, V., Sharpe, S., and Zolla-Pazner, S. (1989) *Proc. Natl. Acad. Sci. U. S. A.* **86**, 1624–1628
32. Varthakavi, V., Browning, P. J., and Spearman, P. (1999) *J. Virol.* **73**, 10329–10338
33. Roos, J. W., Maughan, M. F., Liao, Z., Hildreth, J. E., and Clements, J. E. (2000) *Virology* **273**, 307–315
34. Aiken, C. (1997) *J. Virol.* **71**, 5871–5877
35. Mehle, A., Strack, B., Ancuta, P., Zhang, C., McPike, M., and Gabuzda, D. (2004) *J. Biol. Chem.* **279**, 7792–7798
36. Bardy, M., Gay, B., Pebernard, S., Chazal, N., Courcoul, M., Vigne, R., Decroly, E., and Boulanger, P. (2001) *J. Gen. Virol.* **82**, 2719–2733
37. Bouyac, M., Courcoul, M., Bertoia, G., Baudat, Y., Gabuzda, D., Blanc, D., Chazal, N., Boulanger, P., Sire, J., Vigne, R., and Spire, B. (1997) *J. Virol.* **71**, 9358–9365
38. Huvent, I., Hong, S. S., Fournier, C., Gay, B., Tournier, J., Carriere, C., Courcoul, M., Vigne, R., Spire, B., and Boulanger, P. (1998) *J. Gen. Virol.* **79**, 1069–1081
39. Henderson, L. E., Sowder, R. C., Copeland, T. D., Oroszlan, S., and Benveniste, R. E. (1990) *J. Med. Primatol.* **19**, 411–419
40. Erickson-Viitanen, S., Manfredi, J., Viitanen, P., Tribe, D. E., Tritch, R., Hutchison, C. A., III, Loeb, D. D., and Swanstrom, R. (1989) *AIDS Res. Hum. Retroviruses* **5**, 577–591
41. Pettit, S. C., Moody, M. D., Wehbie, R. S., Kaplan, A. H., Nantermet, P. V., Klein, C. A., and Swanstrom, R. (1994) *J. Virol.* **68**, 8017–8027
42. Wiegers, K., Rutter, G., Kottler, H., Tessmer, U., Hohenberg, H., and Krausslich, H. G. (1998) *J. Virol.* **72**, 2846–2854
43. Conticello, S. G., Harris, R. S., and Neuberger, M. S. (2003) *Curr. Biol.* **13**, 2009–2013
44. Ohagen, A., and Gabuzda, D. (2000) *J. Virol.* **74**, 11055–11066
45. Hoglund, S., Ohagen, A., Lawrence, K., and Gabuzda, D. (1994) *Virology* **201**, 349–355
46. Willey, R. L., Smith, D. H., Lasky, L. A., Theodore, T. S., Earl, P. L., Moss, B., Capon, D. J., and Martin, M. A. (1988) *J. Virol.* **62**, 139–147

Available online at www.sciencedirect.com

SCIENCE DIRECT®

ELSEVIER

Virology 325 (2004) 1–10

VIROLOGY

www.elsevier.com/locate/yviro

Paramyxovirus Sendai virus-like particle formation by expression of multiple viral proteins and acceleration of its release by C protein

Fumihiro Sugahara,[a] Tsuneo Uchiyama,[b] Hitoshi Watanabe,[a] Yukie Shimazu,[a] Masaru Kuwayama,[a] Yutaka Fujii,[a] Katsuhiro Kiyotani,[a] Akio Adachi,[b] Nobuoki Kohno,[c] Tetsuya Yoshida,[a] and Takemasa Sakaguchi[a,*]

[a] *Department of Virology, Graduate School of Biomedical Sciences, Hiroshima University, Hiroshima 734-8551, Japan*
[b] *Department of Virology, Graduate School of Medicine, Tokushima University, Tokushima 770-8503, Japan*
[c] *Department of Molecular and Internal Medicine, Graduate School of Biomedical Sciences, Hiroshima University, Hiroshima 734-8551, Japan*

Received 17 February 2004; returned to author for revision 22 March 2004; accepted 10 April 2004

Abstract

Envelope viruses maturate by macromolecule assembly and budding. To investigate these steps, we generated virus-like particles (VLPs) by co-expression of structural proteins of Sendai virus (SeV), a prototype of the family Paramyxoviridae. Simultaneous expression of matrix (M), nucleo- (N), fusion (F), and hemagglutinin-neuraminidase (HN) proteins resulted in the generation of VLPs that had morphology and density similar to those of authentic virus particles, although the efficiency of release from cells was significantly lower than that of the virus. By using this VLP formation as a model of virus budding, roles of individual proteins in budding were investigated. The M protein was a driving force of budding, and the F protein facilitated and the HN protein suppressed VLP release. Either of the glycoproteins, F or HN, as well as the N protein, significantly shifted density of VLPs to that of virus particles, suggesting that viral proteins bring about integrity of VLPs by protein–protein interactions. We further found that co-expression of a nonstructural protein, C, but not V, enhanced VLP release to a level comparable to that of virus particles, demonstrating that the C protein plays a role in virus budding.

Keywords: Sendai virus; Virus-like particle; Morphology; Density; Nucleocapsid; C protein

Introduction

Sendai virus (SeV), a prototype of the family Paramyxoviridae, is an enveloped virus with a nonsegmented negative-strand RNA genome. The SeV virion has two spike glycoproteins on the lipid-containing envelope, the hemagglutinin-neuraminidase (HN) protein and the fusion (F) protein. Lying underneath the envelope is the matrix (M) protein, which bridges the viral glycoproteins and the internal nucleocapsid. The nucleocapsid has a helical structure consisting of genomic RNA enwrapped with the nucleocapsid (N) protein, associated with RNA polymerase subunits, the large (L) protein, and the phosphoprotein (P). Besides these structural proteins, the P gene encodes the C proteins and the V protein. The C proteins are a generic name of four proteins, C′, C, Y1, and Y2, formed by the various start codons and the common stop codon in a reading frame shifted from that of the P protein. The V protein is synthesized from an accessory mRNA generated by RNA editing during transcription and containing an insertion of a pseudotemplated G residue at a specific editing site. These proteins are not basically incorporated into virions and are termed nonstructural proteins (Lamb and Kolakofsky, 2001; Nagai, 1999). SeV replicates in the cytoplasm and is released from infected cells by assembly and budding at the plasma membrane. Although the current model for assembly of the paramyxovirus implicates the M protein as the principal component promoting the budding of the virus particle (Peeples, 1991; Yoshida et al., 1976, 1979), the underlying mechanism of virion formation is still poorly understood.

Previous studies on retroviruses using the virus-like particle (VLP) system have made great progress in identification of functional domains for budding in the gag protein and in elucidation of their budding mechanisms (Accola et al., 2000; reviewed in Freed, 2002). In the VLP system, the

* Corresponding author. Fax: +81-82-257-5159.
E-mail address: tsaka@hiroshima-u.ac.jp (T. Sakaguchi).

0042-6822/$ - see front matter © 2004 Elsevier Inc. All rights reserved.
doi:10.1016/j.virol.2004.04.019

gag protein is released into the culture medium when expressed in the absence of other viral proteins, forming VLPs that resemble virus particles (Freed, 2002). In negative-strand RNA viruses, M protein-deficient viruses have been generated by using the virus recovery system from cDNA in rabies virus (Mebatsion et al., 1996), measles virus (Cathomen et al., 1998), and SeV (Inoue et al., 2003a). These viruses are invariably defective in virus budding. Furthermore, expression of the M protein or its analogs in the absence of other viral proteins leads to its release into the medium in a lipid-containing vesicle, as was observed for the M protein of vesicular stomatitis virus (VSV) (Justice et al., 1995; Li et al., 1993; Sakaguchi et al., 1999), M1 of influenza virus (Gomez-Puertas et al., 2000; Latham and Galarza, 2001), and VP40 of Ebola virus (Harty et al., 2000; Timmins et al., 2001). In VSV and Ebola virus, ca. 20–40% of the M protein synthesized in cells was released into the medium (Justice et al., 1995; Sakaguchi et al., 1999; Timmins et al., 2001). The M protein of parainfluenzavirus type 1 (PIV1), a paramyxovirus belonging to the same genus Respirovirus as SeV, is also released into the culture medium when expressed alone (Coronel et al., 1999). Co-expression of M and N proteins causes release of vesicles enclosing nucleocapsid-like structures (Coronel et al., 1999). It has also been shown that expression of the SeV M protein results in its release from cells (Sakaguchi et al., 1999; Takimoto et al., 2001). Moreover, the F protein as well as the M protein has been shown to form vesicles to be released when expressed alone, and protein motifs necessary for the release, including putative actin-binding motifs, have been identified (Takimoto et al., 2001). However, a quantitative study on the release has not been performed.

Schmitt et al. (2002) generated VLPs that resembled authentic virus particles by expressing proteins of simian virus 5 (SV5), a member of the genus Rubulavirus of the family Paramyxoviridae, and demonstrated that expression of the M protein alone was not sufficient for its release from cells but that simultaneous expression of the M protein, N protein, and one of the viral glycoproteins, F and HN proteins, was necessary for efficient VLP release from cells. The results of that study show that interactions among multiple viral proteins, not the M protein alone, confer budding competence on VLP, suggesting a different mechanism of paramyxovirus budding.

To further clarify the mechanism of paramyxovirus assembly and budding by using a VLP system, it is important to investigate the effects of other viral proteins, in addition to the M protein, on VLP formation. In the present study, we generated VLPs by co-expressing SeV proteins in various combinations, and we evaluated the contribution of each viral protein to budding by quantifying VLP release from cells. Furthermore, roles of each viral protein in VLP formation towards an authentic virus particle were also investigated by estimating density of the VLPs and by electron microscopy. The results showed that the M protein was indeed a major driving force of SeV budding and that the F and HN proteins had enhancing and suppressive effects on budding, respectively. Furthermore, we show that the four viral proteins M, N, F, and HN, are required for formation of VLPs with density and morphology similar to those of authentic SeV particles and that the C protein enhances VLP release.

Results

VLP formation by expression of SeV M, N, F, and HN proteins

SeV M, N, F, and HN proteins were simultaneously expressed in 293T cells and metabolically labeled with [^{35}S]cysteine and [^{35}S]methionine. The culture medium was then collected and directly fractionated by sucrose floatation ultracentrifugation. Viral proteins in the floated fraction showed that these four proteins were released in the form of lipid-containing vesicles (Fig. 1A). Viral proteins in the cells were also analyzed, and the fraction of the released M protein was calculated as described in Materials and methods. The released fraction was 3.6% which was ca. 1/5 of that of virus particles from infected cells (18.3%) (Fig. 1A).

Sucrose density equilibrium ultracentrifugation of the culture supernatant demonstrated that the M, N, F, and HN proteins were concentrated to fraction 14 (density = 1.17–1.20 g/ml), which was identical to that of authentic virus particles (Fig. 1B). Electron microscopy with negative staining showed the existence of virus-like particles (VLPs) that appeared to be similar to authentic virus particles (Fig. 1C). Herring bone-like, nucleocapsid-like structures were also found beside the VLPs (Fig. 1C). This finding is consistent with a previously reported finding that expression of the SeV N protein in cells resulted in generation of nucleocapsid-like structures (Buchholz et al., 1993). The VLPs seem to contain RNA actually because radioactivity was found at fractions 14–16 in [^{3}H]uridine labeling (data not shown). These results indicate that simultaneous expression of the M, N, F, and HN proteins yielded VLPs with morphology and density similar to those of actual virus particles, suggesting that VLP formation can be a model for virus budding. The release efficiency of the VLPs was, however, significantly lower than that of SeV from infected cells.

Amounts of the N protein in the VLPs and virus particles were compared with those of other viral proteins after sucrose density equilibrium ultracentrifugation. Ratios of N protein to M protein in fraction 14 in Fig. 1B were 1.6 for the VLP and 0.7 for the SeV particle. The VLP was shown to contain more N proteins than the amount in the SeV particle. The ratios of other proteins in VLPs and SeV particles appeared to be similar.

We added an exogenous neuraminidase to the medium to prevent VLPs from being trapped on the cell surface by the

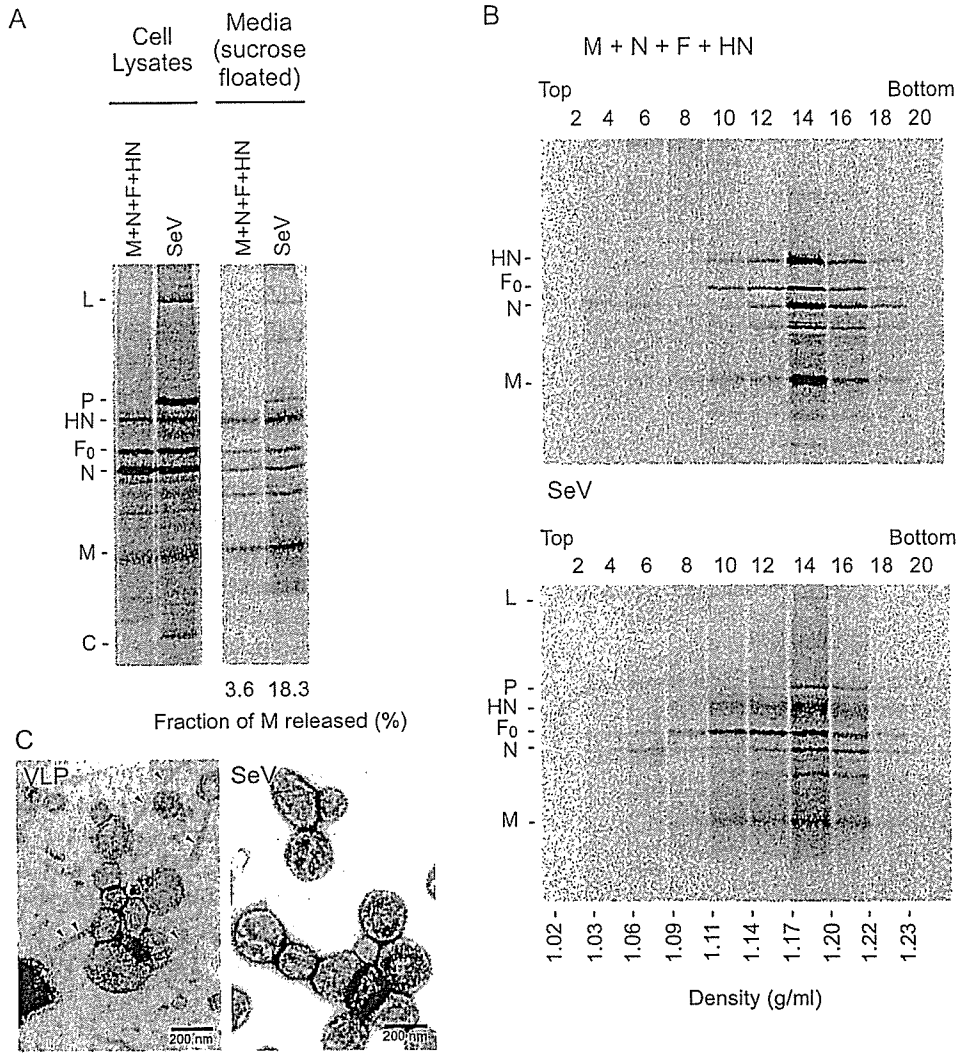

Fig. 1. Comparison of VLPs by co-expression of M, N, F, and HN proteins and SeV. (A) 293T cells were transfected with plasmids for expression of M, N, F, and HN proteins or infected with SeV at an m.o.i. of 10 and labeled with [^{35}S]cysteine and [^{35}S]methionine from 24 to 48 h post-transfection. The medium was then separated by sucrose floatation ultracentrifugation, and proteins in the floated fraction were analyzed by immunoprecipitation and SDS-PAGE. Proteins in the cells were also analyzed, and the released fraction of the M protein is shown in the figure. F_0: precursor of the F protein before proteolytic processing. Proteins from 1/15 of the cell lysates and those from half of the medium were run in a lane. (B) The medium from the labeled cells was then separated by sucrose density equilibrium ultracentrifugation in a 20–50% continuous gradient. Fractions were collected, and SeV proteins in each fraction were analyzed by immunoprecipitation and SDS-PAGE. Density of fractions was measured by weighing each fraction. (C) The medium from transfected 293T cells was concentrated by ultracentrifugation at 24000 rpm for 1 h through a 7% (w/w) sucrose cushion. The pellet was then suspended in PBS, processed for negative staining, and observed by electron microscopy. Arrowheads indicate nucleocapsid-like structures.

hemagglutinating activity. The addition improved VLP release by ca. 2-fold in some experiments, although it was not always reproducible. The medium was supplemented with neuraminidase in all of the experiments in this study.

Contribution of each SeV protein to VLP release from cells

We investigated the role of each SeV protein in VLP formation. Expression of the M protein alone led to an efficient release of M proteins into the medium (Fig. 2A). The efficiency of the M protein release was calculated to be 14.5%. The F protein was also released but with less efficiency (0.7%) (Fig. 2A). Only a trace amount of proteins was released when either the N or HN protein was expressed (Fig. 2A).

Expression of the F protein with the M protein increased the released fractions of both proteins, especially that of the F protein significantly (from 0.7% to 6.5%) (Fig. 2B), suggesting a synergic effect of protein release. In contrast, expression of the HN protein with the M protein resulted in suppression of M protein release (from 14.5% to 0.6%), although the released fraction of the HN protein itself was slightly increased from 0.1% to 0.4%. Expression of the N protein with the M protein also decreased the released fraction of the M protein to 3.2%, while it increased the released fraction of the N protein from 0.03% to 0.4% (Fig.

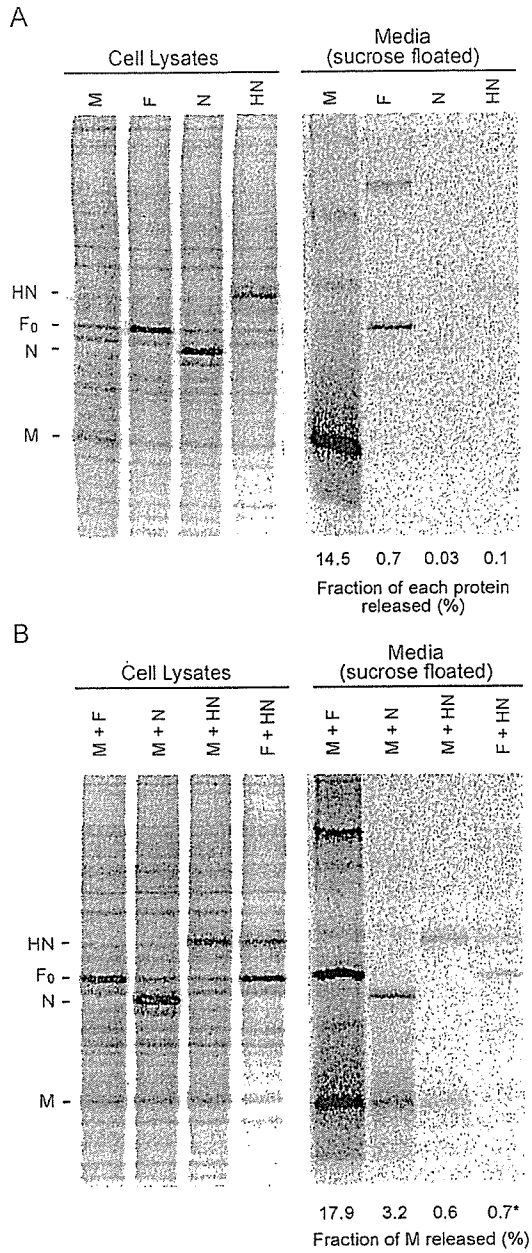

Fig. 2. Protein release by expression of single or double SeV proteins. A single plasmid (A) or two plasmids (B) as indicated in the figure were introduced into 293T cells and labeled with [^{35}S]cysteine and [^{35}S]methionine from 24 to 48 h post-transfection. The vesicles released were concentrated by sucrose floatation ultracentrifugation, and proteins were analyzed by immunoprecipitation and SDS-PAGE. Proteins in the cells were also analyzed, and protein release was calculated by each protein (A) and by the M protein (B). Asterisk: protein release was calculated by the HN protein. Proteins from 1/15 of the cell lysates and those from half of the medium were run in a lane in these gels.

2B). HN and N proteins could be a burden for M-driven vesicle release. Co-expression of the two glycoproteins, F and HN, did not result in efficient release of these proteins (Fig. 2B).

An apparent constant intracellular level of the M protein in Fig. 2B does not seem to accord with the fact that the released fraction of M protein varied from 0.6% to 17.9%; intracellular M protein level should vary in accordance with the variation in the released fraction. This is due to the sample amount loaded on the gel as described in Materials and methods (1/15 of the cell lysates and half of the medium). The difference between the amounts of M proteins in cells was therefore compressed to 1/7.5, making it difficult to detect the difference between levels of intracellular M protein.

Expression of the M, N, F, and HN proteins resulted in formation of a VLP as described above. Removal of the M protein from this combination resulted in complete suppression of VLP release, supporting the notion that the M protein is a major driving force for release (Fig. 3A). Removal of the F protein also reduced the released proteins to 0.5%, indicating that the F protein has a release-promoting effect (Fig. 3A). Removal of the N protein did not significantly affect the efficiency of release in this case (Fig. 3A). It is notable that without the HN protein, release of the remaining proteins, M, F, and N proteins, was enhanced (8.3%; Fig. 3A). An increase in amounts of transfected HN plasmids resulted in greater suppression of VLP release (Fig. 3B), confirming that the HN protein has an inhibitory effect on release. The inhibitory effect may not be due to cell toxicity of the HN protein because viral protein synthesis appeared to be constant in the transfected cells (Fig. 3B) and no apparent CPE was observed (data not shown). For experiments in this study, 0.5 μg of the HN plasmid was used to adjust the intracellular expression level of HN protein to that in SeV-infected cells.

Acceleration of VLP release by co-expression of the C protein

Effects of nonstructural proteins, C and V proteins, on the VLP release were further examined. Expression of the C protein together with M, N, F, and HN proteins enhanced VLP release by more than 2-fold (Fig. 4). The enhancement was highly reproducible (Fig. 4), showing that the C protein increased the efficiency of VLP release. In contrast, the V protein did not have such an enhancing activity (data not shown). The fraction of M released into VLPs formed by M, N, F, HN, and C was 9.8%, almost half of the M fraction released into SeV particles (Fig. 4).

Density and morphology of structures released by expression of viral proteins in various combinations

We performed sucrose density equilibrium ultracentrifugation to determine the density of released proteins. M protein released by single expression showed a wide range of densities, indicating heterogeneity of M protein-containing structures (Fig. 5). The M protein was found in abundance in fractions 8 to 16 (1.09–1.22 g/ml). The M protein was considered to be released in association with

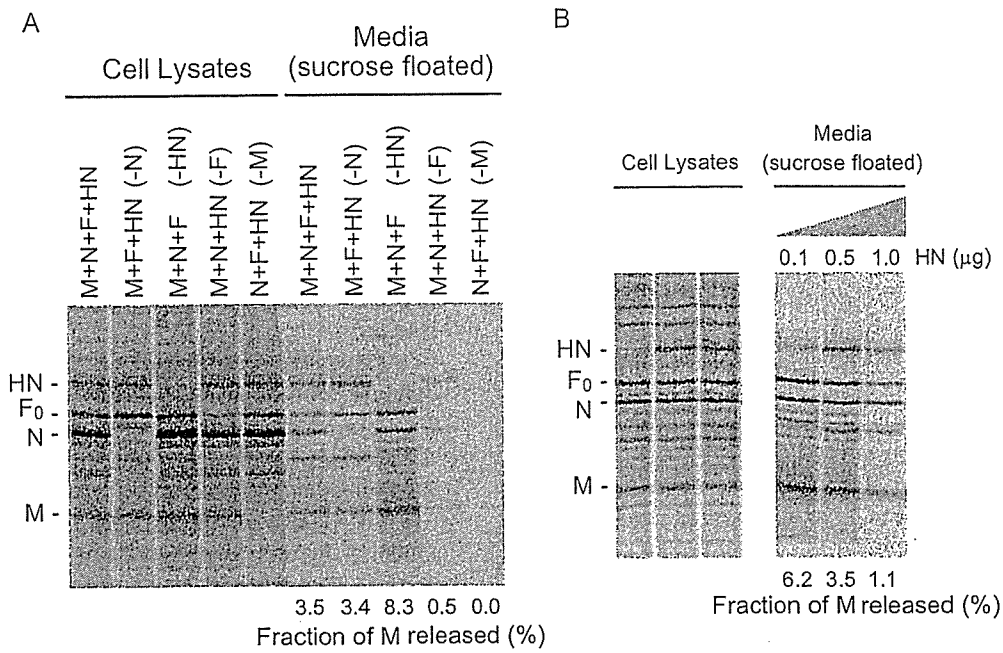

Fig. 3. (A) Contribution of SeV proteins to VLP release from cells. 293T cells were transfected with multiple plasmids as indicated in the figure and labeled with [^{35}S]cysteine and [^{35}S]methionine from 24 to 48 h post-transfection. The medium was then separated by sucrose floatation ultracentrifugation, and proteins in the floated fraction were analyzed by immunoprecipitation and SDS-PAGE. Proteins in the cells were also analyzed, and protein release was calculated by the M protein. (B) Effect of the HN protein on VLP release. The M, N, and F plasmids together with increasing amounts of the HN plasmid were introduced into 293T cells, and proteins were analyzed. Proteins from 1/15 of the cell lysates and those from half of the medium were run in a lane in these gels.

lipids because treatment with 1% Triton X-100 before ultracentrifugation shifted the distribution (data not shown). The singly expressed F protein was distributed in a narrow range around fraction 14 (1.17–1.20 g/ml) (Fig. 5), and released N protein was slightly detected in a heavier fraction, fraction 16 (1.20–1.22 g/ml) (Fig. 5).

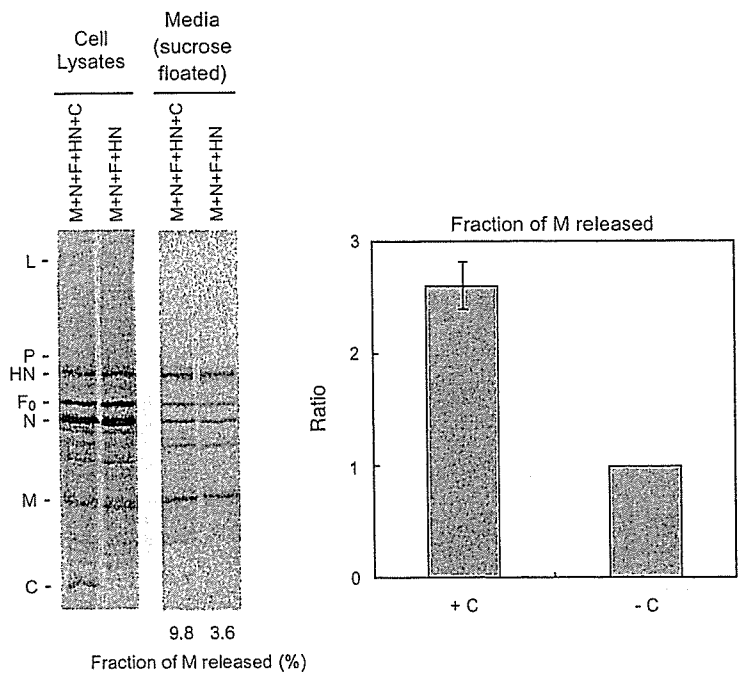

Fig. 4. Effect of C protein on VLP release from cells. 293T cells were transfected with multiple plasmids with or without the C plasmid as indicated in the figure and labeled with [^{35}S]cysteine and [^{35}S]methionine from 24 to 48 h post-transfection. The medium was then separated by sucrose floatation ultracentrifugation, and proteins in the floated fraction were analyzed by immunoprecipitation and SDS-PAGE. Proteins in the cells were also analyzed similarly, and protein release was calculated by the M protein. Proteins from 1/15 of the cell lysates and those from half of the medium were run in a lane. The graph indicates the ratio of fractions of M released into VLPs from four independent experiments. Error bar indicates standard deviation.

When the F protein was expressed with the M protein, these two proteins co-existed mainly in fractions 12 and 14 (Fig. 5, M + F). The distribution of the M protein was shifted into these fractions (Fig. 5, M + F). A band between the M and F_0 proteins was considered to be β-actin because it reacted with anti-β-actin antibody in immunoblotting (data not shown) as described previously (Takimoto et al., 2001). Expression of the N protein with the M protein resulted in co-existence of N and M proteins in a fraction similar to that when the N protein was singly expressed (Fig. 5, M + N). On the other hand, a significant amount of the M protein was found in fractions 8–12 (Fig. 5, M + N), probably having been released independently of the release of the N protein. The changes in distribution and amounts of released proteins by co-expression suggest interactions between F and M proteins and between M and N proteins. In contrast, simultaneous expression of F and N proteins caused no change in protein release or in density distribution compared with those in the case of single expressions (data not shown).

Triple expression of M, N, and F proteins caused co-localization of these three proteins in fraction 14, suggesting that a significant amount of these proteins interacted and formed VLPs with density similar to that of authentic virus particles (Fig. 5, M + N + F). On the other hand, some N proteins were found in a heavier fraction, fraction 18, and some F_0 proteins were found in the lighter fractions, fractions 10 and 12, suggesting that some proteins were independently released probably in heterogeneous VLPs. Triple expression of M, N, and HN proteins caused less VLP release in total, but the proteins were fairly concentrated to fraction 14 (Fig. 5, M + N + HN). The glycoproteins F and HN appeared to guide M and N proteins to fraction 14.

Simultaneous expression of M, N, F, and HN proteins resulted in concentration almost all of these proteins to fraction 14, suggesting formation of homogenous VLPs with density similar to that of virus particles (Fig. 1B). Additional expression of the C protein with the four proteins did not alter the distribution of the proteins, although amounts of the proteins were increased overall (data not shown). Convergence by co-expression of viral proteins to fraction 14, which had the same density as SeV particles, was apparent when the percent distribution of the M protein was plotted in a graph (Fig. 5).

Negative staining and electron microscopy demonstrated that the supernatant from the cells expressing only the M

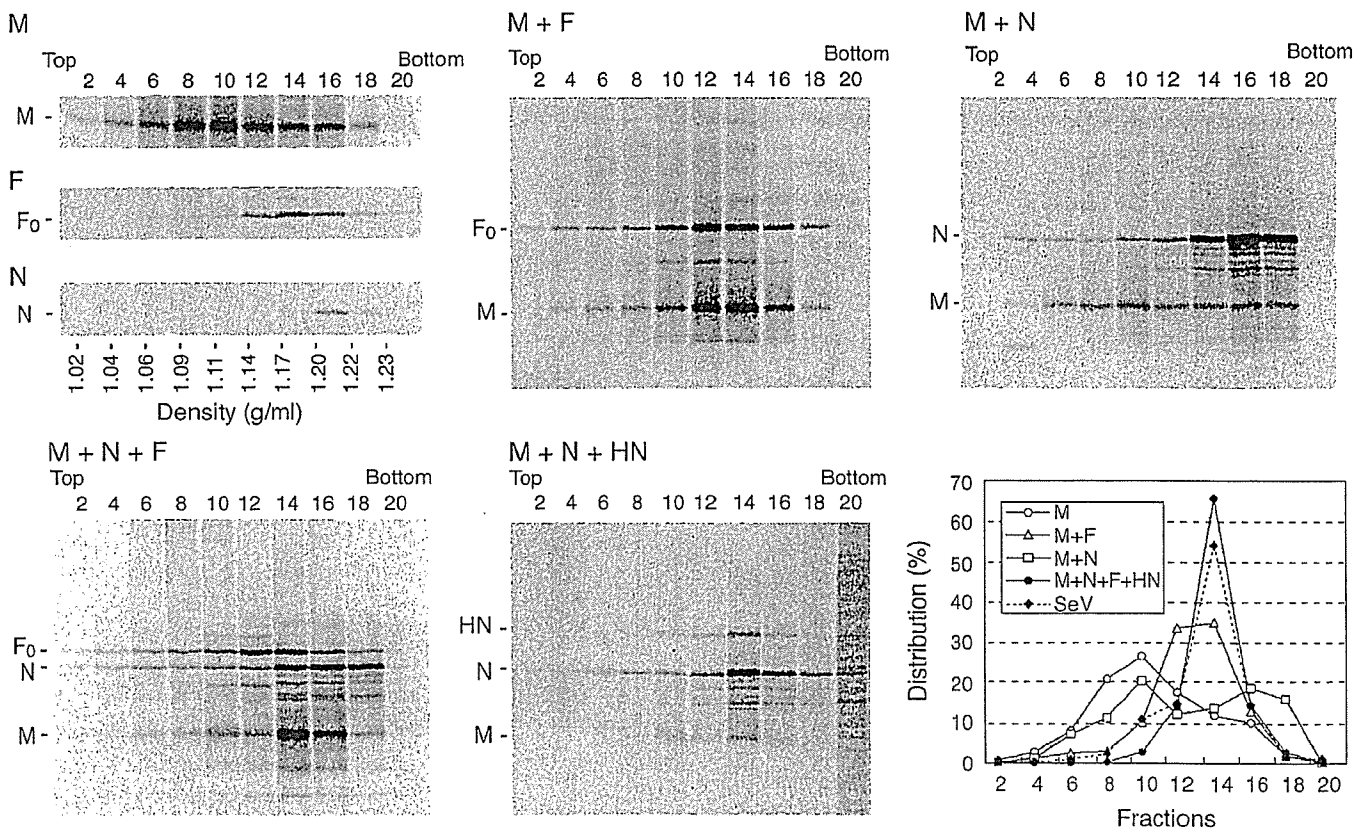

Fig. 5. Distributions of densities of VLPs with an increasing number of plasmids. Plasmids for expression of a single viral protein (M, F, or N) or those for expression of multiple viral proteins (M + F, M + N, M + N + F, or M + N + HN) were introduced into 293T cells and labeled with [^{35}S]cysteine and [^{35}S]methionine from 24 to 48 h post-transfection. The medium was then separated by sucrose density equilibrium ultracentrifugation in a 20– 50% continuous gradient. Fractions were taken and SeV proteins in each fraction were analyzed by immunoprecipitation and SDS-PAGE. (Graph) Percent distributions of the M protein in the results from each combination of plasmids in Fig. 1B (M + N + F + HN, SeV) and this figure (M, M + F, M + N) are plotted in a graph.

protein had vesicles with smooth surfaces (Fig. 6A). The vesicles from the cells expressing M and F proteins had rough surfaces with some geometric patterns, indicating the presence of abundant spikes on the surfaces (Fig. 6B). Furthermore, the vesicles formed by M, F, and N proteins had nucleocapsid-like structures inside (Fig. 6C). There were also some structures outside the particles (Fig. 6C). Co-expression of M, N, F, and HN proteins generated VLPs similar to virus particles (Fig. 1C), although small vesicles were also seen in the VLPs (data not shown). There was no difference between the morphology of VLPs generated by co-expression of M, N, F, and HN proteins with the C protein and that without the C protein (data not shown).

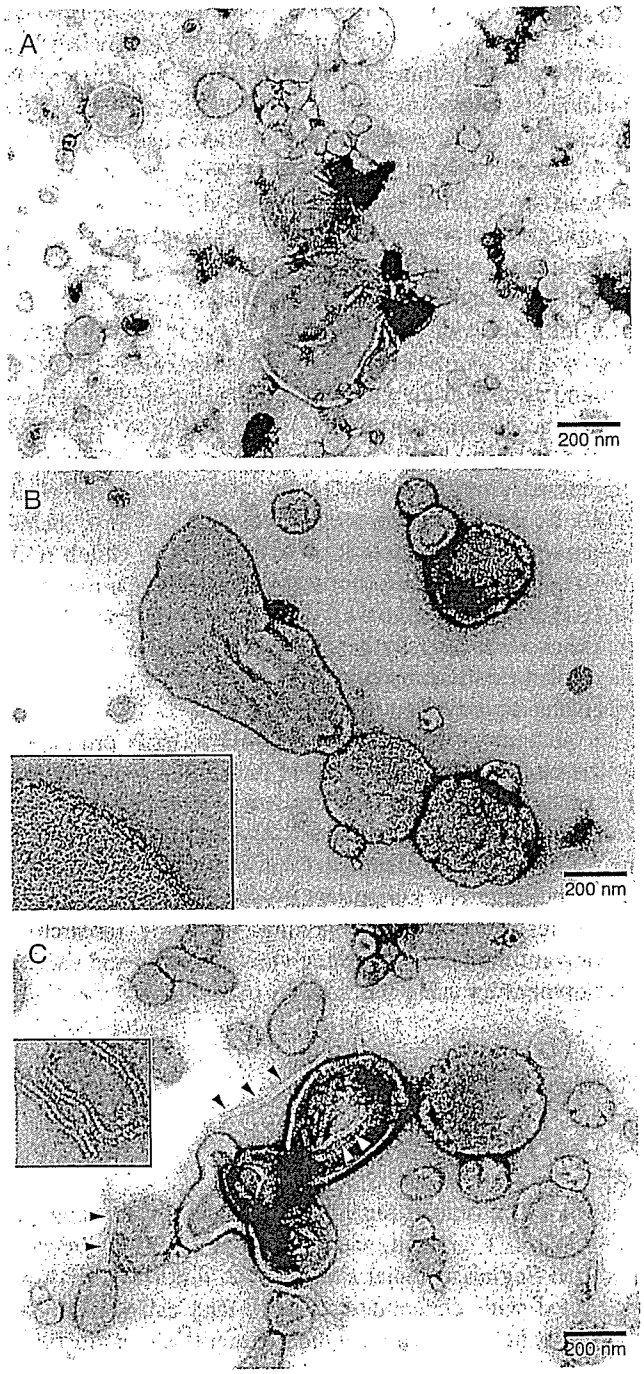

Fig. 6. Electron microscopy of structures released from transfected cells. The medium from transfected 293T cells was clarified by low-speed centrifugation, passed through a 5-μm filter, and centrifuged at 24 000 rpm for 1 h through a 7% (w/w) sucrose cushion. The pellet was resuspended in PBS, processed for negative staining, and observed by electron microscopy. (A) Single expression of M. (B) Double expression of M and F. (Inlet) Magnification of the surface of the VLP. (C) Triple expression of M, N, and F. Arrowheads indicate nucleocapsid-like structures. (Inlet) Magnification of the nucleocapsid-like structures.

Discussion

In the present study, we expressed SeV proteins and produced VLPs. Co-expression of M, N, F, and HN proteins and sucrose density equilibrium ultracentrifugation concentrated these proteins into a common fraction, to which the authentic virus particles migrated, indicating that these proteins autonomously assembled into VLPs that are comparable to the authentic virus particles in terms of density. The similar densities seem to reflect the common compositions of the virus particles and the VLPs. The VLP formation can thus be used as a model for virus assembly and budding. In this condition, however, protein release was only one-fifth of that of SeV. A higher level of release, almost half of the efficiency of SeV, was obtained by co-expression of C protein together with M, N, F, and HN proteins. To get closer the efficiency of VLP release to that of virus release, some other viral proteins or the nucleocapsid containing the full-length genomic RNA might be necessary.

Schmitt et al. (2002) expressed multiple proteins of SV5, a paramyxovirus classified to the genus distinct from that of SeV, in 293T cells to generate VLPs (Schmitt et al., 2002). The study shows that the M protein alone does not result in generation of VLPs from cells, but co-expression of the N protein and one of the glycoproteins, F or HN protein, together with the M protein is necessary for efficient VLP budding. This situation is different from that of SeV. Furthermore, the glycoproteins, F and HN proteins, have similar budding-promoting effects in SV5, whereas in SeV, the F protein was promoting and the HN protein was inhibitory for VLP budding. The differences revealed by VLP formation may indicate differences of mechanism of virus budding between SV5 and SeV.

An intracellular nucleocapsid structure formed by single expression of the N protein has been reported in paramyxoviruses: SeV (Buchholz et al., 1993), measles virus (Spehner et al., 1991), and Newcastle disease virus (Errington and Emmerson, 1997). Once formed in cells, the nucleocapsid-like structure could be a substitute for the nucleocapsid in VLP budding. We found that the ratio of the N protein to other viral proteins in VLPs was different to that in the virus particles; the ratios of the N protein to the M protein were 1.6:1 in VLPs and 0.7:1 in the virus particles.

The N protein in VLPs appeared to be more abundant than that in the virus, as had been observed in VLP formation in SV5 (Schmitt et al., 2002). The VLPs may contain nucleocapsid-like structures of various lengths, almost all of which are probably shorter than the viral nucleocapsid (15384 bases). Such differences in length may affect the N protein ratio because difference in length affects the nucleocapsid incorporation and budding as shown by using defective interfering particles (Mottet and Roux, 1989).

Interaction between the M protein and viral glycoproteins has been shown by using biochemical and cell biological methods (Yoshida et al., 1976, 1979, 1986) and by the use of live viruses whose cytoplasmic tails of the glycoproteins were deleted (Fouillot-Coriou and Roux, 2000). Recently, Ali and Nayak (2000) showed the interaction of M and glycoproteins in a raft domain by solubilizing cells with a nonionic detergent and a subsequent sucrose floatation. The shift of fractions observed in the sucrose density ultracentrifugation of VLPs suggested the interaction. On the other hand, Takimoto et al. (2001) did not suggest the interaction, based on the observation that the co-expressed and released M and F proteins were in distinct fractions after sucrose density equilibrium ultracentrifugation, although they suggested a functional interaction by release acceleration of both of the proteins. The reason for the contradiction with ours is unknown. The present study also suggested protein–protein interaction between M and N. This is consistent with the previous reports (Coronel et al., 1999, 2001; Yoshida et al., 1976).

Fouillot-Coriou and Roux (2000) showed by using recombinant SeVs possessing cytoplasmic tail-deleted glycoproteins that a partial deletion of the F tail caused the virus to bud inefficiently, while the rates of incorporation of the F protein to other viral proteins were almost constant. It seems that the F protein is essential for virus budding, as if it is a part of the budding machinery. On the other hand, the tail-less HN basically had no effect on virus budding, and HN mutants are not incorporated in some cases in a cytoplasmic motif-dependent fashion (Fouillot-Coriou and Roux, 2000; Takimoto et al., 1998). Furthermore, efficient budding of an HN-deficient SeV has been reported (Inoue et al., 2003b; Leyrer et al., 1998; Stricker and Roux, 1991). These results suggest that SeV F and HN proteins have different roles in virus budding. Our study showed that the F protein had a promoting effect on VLP budding, while the HN protein had an inhibitory effect. Although Takimoto et al. (2001) demonstrated that the HN protein did not have such an inhibitory effect on M-driven vesicle release, the reason of the discrepancy is not known. The HN protein increased VLPs of uniform density (Fig. 5) and may have enhanced the integrity of VLPs.

Hasan et al. (2000) reported that SeV lacking all of the four C proteins yielded less virus particles and that the particles were irregular in shape, suggesting a role of the C protein in virus assembly and budding. In the present study, addition of the C protein to the VLP system enhanced VLP release from cells. This is strong evidence that a paramyxovirus accessory protein affects virus budding. In infected cells, the exogenous C protein has a suppressive effect on RNA synthesis (Curran et al., 1992; Horikami et al., 1997). Thus, the function of the C protein in virus budding had been difficult to analyze in virus-infected cells. The present VLP system could illustrate the action of the C protein on virus budding. However, the mechanism of acceleration of VLP release by the C protein is unknown and to be resolved. The C protein is known to co-localize with the M and HN proteins in infected cells (Hasan et al., 2000), and it is thought that the C protein acts as a molecular chaperon to facilitate assembly of viral proteins by interacting with M protein. Although the C protein has been shown to interact with the L protein (Horikami et al., 1997), the interaction may not be involved in VLP release because the VLP-forming system in the present study lacked the L protein.

The acceleration of VLP release by the C protein is limited to only 2- to 3-fold, while a C-knockout virus suppressed virus formation by ca. 100-fold (Hasan et al., 2000). Because the C protein has various functions, including anti-interferon activity (Garcin et al., 1999; Gotoh et al., 1999) and inhibition of viral RNA synthesis (Curran et al., 1992; Horikami et al., 1997), the extremely low yield of C-knockout virus may be due to the summation of impediments of these functions in addition to that of the budding-enhancing activity identified in this work.

In summary, we have established a VLP production system of SeV. The generated VLPs had density similar to that of actual virus particles, and the released VLPs were comparable to the virus particles. A novel finding by using the VLP system was that the C protein directly facilitated virus budding. The current VLP system will be useful in further research on virus budding, including research to develop antiviral drugs targeting virus assembly and vaccine development by using VLPs as an immunogen.

Materials and methods

Cells and a virus

293T cells, human renal epithelial cells expressing the SV40 large T antigen, were propagated in Dulbecco's modified Eagle's minimal essential medium (DMEM) supplemented with glutamine and 10% fetal calf serum. Recombinant SeV derived from the Z strain (Kato et al., 1996) was propagated in embryonated chicken eggs as described previously (Kiyotani et al., 1990).

Plasmids

The plasmids, pCAGGS-M, pCAGGS-N, pCAGGS-F and pCAGGS-HN, for mammalian expression of SeV proteins under the chicken β-actin promoter (Niwa et al., 1991) were described previously (Sakaguchi et al., 1999).

The expression plasmid for the C protein, pCAGGS-C, was constructed in this study.

Transfection, infection, and metabolic labeling

Subconfluent 293T cells were transfected with plasmids by using the FuGENE6 transfection reagent (Roche Diagnostics, Indianapolis, IN). For a 60-mm dish, 3.5 μg of plasmids were used in cotransfection experiments: pCAGGS-M, 1 μg; pCAGGS-F, 1 μg; pCAGGS-N, 0.5 μg; pCAGGS-HN, 0.5 μg; pCAGGS-C, 0.5 μg. The plasmid amounts were determined so that intracellular levels of protein expression were similar to those in virus-infected cells. In the case of omission of an expression plasmid, a vector plasmid, pCAGGS, was added to keep the total amount of transfected DNA constant. For a 100-mm dish, a 3-fold larger amount of the plasmids was used. Alternatively, 293T cells were infected with SeV at an m.o.i. of 10.

For metabolic labeling of viral proteins, the medium of transfected or infected 293T cells was replaced with 1.5 ml of DMEM containing one-tenth of the normal amounts of cysteine and methionine and 2.5 MBq/ml of [^{35}S]cysteine and [^{35}S]methionine mixture ([^{35}S]Pro-mix, Amersham Biosciences, Piscataway, NJ), together with 10 mU of bacterial neuraminidase (Roche Diagnostics) after 24 h. After 48 h, the medium and cells were collected separately.

Sucrose floatation and sucrose density equilibrium ultracentrifugation

For a sucrose floatation assay, the medium was clarified by centrifugation at 7000 rpm for 5 min, and 1.4 ml of the supernatant was mixed with 2.1 g sucrose to adjust its concentration to 60% (w/w). The supernatant was then transferred to a centrifuge tube, overlaid with 7 ml of 50% (w/w) sucrose/phosphate-buffered saline (PBS) and 0.5 ml of 10% (w/w) sucrose/PBS, and centrifuged at 35000 rpm for 18 h in a RPS40T rotor (Hitachi, Tokyo, Japan). The top 1.5-ml fraction including the 10% and 50% sucrose boundary was collected and solubilized in a radioimmunoprecipitation assay (RIPA) buffer [10 mM Tris–HCl, pH 7.4, 1% Triton X-100, 1% sodium deoxycholate, 0.1% sodium dodecyl sulfate (SDS), and 150 mM NaCl] containing 50 mM iodoacetamide (IAA) and 1 mM phenylmethylsulfonyl fluoride (PMSF). Cells were solubilized in a RIPA buffer containing IAA and PMSF and then centrifuged at 15000 rpm for 20 min to remove nuclei and cell debris.

For sucrose density equilibrium ultracentrifugation, the medium was clarified at 7000 rpm for 5 min and was layered onto the top of a 20–50% sucrose/PBS linear density gradient and centrifuged at 35000 rpm for 18 h in a RPS40T rotor. Fractions were obtained by using an Auto Densi-Flow fractionator (Labconco, Kansas City, MO). Density of fractions was measured by weighing each fraction. Proteins in the fractions were solubilized by adding concentrated RIPA buffer containing IAA and PMSF.

Immunoprecipitation and SDS-PAGE

Solubilized proteins in the RIPA buffer were mixed with 2 μl of anti-SeV serum, 1 μl of anti-C serum (kindly provided by A. Kato), and 30 μl of Protein A Sepharose beads, followed by agitation for 18 h at 4 °C. Immune complexes were washed three times with the RIPA buffer, suspended in SDS sample buffer, and boiled for 3 min as described previously (Sakaguchi et al., 1996). Proteins were analyzed by SDS-polyacrylamide gel electrophoresis (PAGE) using an 11% gel, and protein bands were visualized and quantitated by using a BAS2000 image analyzer (Fuji Film, Tokyo, Japan). The fraction of viral proteins released into the medium was calculated basically as the ratio of the M protein detected in the medium to the total M protein both in the medium and the cells. Proteins from 1/15 of the cell lysates and those from half of the medium were run in a lane in these gels.

Electron microscopy

For electron microscopy, subconfluent 293T cells in 100-mm dishes were transfected with plasmids, and after 48 h, the media were clarified by low-speed centrifugation and passed through a Millex-SV filter with a pore size of 5.0 μm (Millipore, Bedford, MA) to completely remove cells and then pelleted through a 7% (w/w) sucrose/PBS cushion by ultracentrifugation at 24000 rpm for 1 h. The pellet was resuspended in PBS, placed on Formvar-carbon-coated nickel grids, stained with 4% uranyl acetate, and examined under a JEOL JEM-1200EX II transmission electron microscope as described previously (Uchiyama and Uchida, 1988).

Acknowledgments

We thank Yoshiyuki Nagai, Atsushi Kato, and Makoto Inoue for supplying an antibody and for their helpful discussions, and we thank the staff of the Research Center for Molecular Medicine, Hiroshima University School of Medicine, for allowing us the use of their facilities. This work was supported by Grants-in-Aid for Scientific Research from the Japan Society for the Promotion of Science.

References

Accola, M.A., Strack, B., Gottlinger, H.G., 2000. Efficient particle production by minimal Gag constructs which retain the carboxy-terminal domain of human immunodeficiency virus type 1 capsid-p2 and a late assembly domain. J. Virol. 74, 5395–5402.

Ali, A., Nayak, D.P., 2000. Assembly of Sendai virus: M protein interacts with F and HN proteins and with the cytoplasmic tail and transmembrane domain of F protein. Virology 276, 289–303.

Buchholz, C.J., Spehner, D., Drillien, R., Neubert, W.J., Homann, H.E., 1993. The conserved N-terminal region of Sendai virus nucleocapsid